

1970

# The crystal and molecular structures of selected organometallic compounds and some direct methods

Leslie Leon Martin  
*Iowa State University*

Follow this and additional works at: <https://lib.dr.iastate.edu/rtd>

 Part of the [Physical Chemistry Commons](#)

## Recommended Citation

Martin, Leslie Leon, "The crystal and molecular structures of selected organometallic compounds and some direct methods " (1970). *Retrospective Theses and Dissertations*. 4340.  
<https://lib.dr.iastate.edu/rtd/4340>

This Dissertation is brought to you for free and open access by the Iowa State University Capstones, Theses and Dissertations at Iowa State University Digital Repository. It has been accepted for inclusion in Retrospective Theses and Dissertations by an authorized administrator of Iowa State University Digital Repository. For more information, please contact [digirep@iastate.edu](mailto:digirep@iastate.edu).

71-7301

MARTIN, Leslie Leon, 1942-  
THE CRYSTAL AND MOLECULAR STRUCTURES OF  
SELECTED ORGANOMETALLIC COMPOUNDS AND SOME  
DIRECT METHODS.

Iowa State University, Ph.D., 1970  
Chemistry, physical

University Microfilms, Inc., Ann Arbor, Michigan

THE CRYSTAL AND MOLECULAR STRUCTURES OF  
SELECTED ORGANOMETALLIC COMPOUNDS AND SOME DIRECT METHODS

by

Leslie Leon Martin

A Dissertation Submitted to the  
Graduate Faculty in Partial Fulfillment of  
The Requirements for the Degree of  
DOCTOR OF PHILOSOPHY

Major Subject: Physical Chemistry

Approved:

Signature was redacted for privacy.

In Charge of Major Work

Signature was redacted for privacy.

Head of Major Department

Signature was redacted for privacy.

Dean of Graduate College

Iowa State University  
Ames, Iowa

1970

PLEASE NOTE:

Some pages have small  
and indistinct type.  
Filmed as received.

University Microfilms

## TABLE OF CONTENTS

	Page
INTRODUCTION	1
STRUCTURE OF 2[TETRA(TRIMETHYLSILYL)CYCLOHEXENE-1-YL]HEPTAMETHYLTRISILANE	3
Introduction	3
Experimental	3
Results and Discussion	10
STRUCTURE OF <i>cis</i> -DICHLOROBIS(DIMETHYLPHENYLPHOSPHINE) PALLADIUM(II)	23
Introduction	23
Experimental	23
Solution and Refinement of the Structure	26
Description of the Structure	38
Discussion	39
STRUCTURE OF NITRILOTRIACETODIAQUOPRASEODYMIUM(III)-MONOHYDRATE	44
Introduction	44
Experimental	45
Solution of the Structure	47
Results and Discussion	48
STRUCTURE OF NITRILOTRIACETODIAQUODYSPROSIUM(III)-DIHYDRATE	67
Introduction	67
Experimental	67
Solution of the Structure	70
Discussion	81

	Page
THE QUADRUPLE PRODUCT	101
Introduction	101
Description of the Method	103
Application of the Method	110
LITERATURE CITED	115
ACKNOWLEDGMENTS	119
APPENDIX A. A LISTING OF QUADS	120
APPENDIX B. A LISTING OF RELATE	124
APPENDIX C. RESEARCH PROPOSALS	130

## INTRODUCTION

The term "organometallic" is used to describe a wide range of compounds in which the organo-group is bonded directly to a metal atom. In addition, this term is often used to indicate compounds in which the organo-group is bonded to such atoms as silicon, boron, or phosphorus. The four compounds,  $\text{Si}_7\text{C}_{26}\text{H}_{55}$ ,  $\text{Pd}(\text{P}(\text{CH}_3)_2\text{C}_6\text{H}_5)_2\text{Cl}_2$ ,  $\text{Pr}(\text{N}(\text{C}_2\text{H}_2\text{O}_2)_3)3\text{H}_2\text{O}$ ,  $\text{Dy}(\text{N}(\text{C}_2\text{H}_2\text{O}_2)_3)4\text{H}_2\text{O}$  all fall into this category. An attempt was made to select compounds for study for which there was relatively little structural information available or the information was inconclusive and a crystal structure study would remove the ambiguity.

The silicon compound was selected for study due to the dearth of structural information available on multiple Si-Si bonding. In fact, this is, to my knowledge, the first crystal structure report of a compound with multiple Si-Si bonds. The silicon atoms were found to have a normal tetrahedral type configuration with little evidence for d-orbital contribution to the bonding despite the presence of a carbon-carbon double bond adjacent to the trisilane moiety. In the case of the palladium structure, information available on the structure was inconclusive. This study determined the configuration of the compound to be cis, square-planar with a significant lengthening of the Pd-Cl bond and a shortening of the Pd-P bond. The amount of structural information available for the

rare earth complexes is limited; especially on structural changes across an entire series of rare earths complexed to one particular ligand. The purpose of the study of the lanthanon(III)-nitrilotriacetate complexes was to provide good structural information on the nature of the changes in the complexes across the series and to determine the causes of these changes. The two structures, which are presented here, show a gross structural change from nona-coordinate to octa-coordinate with additional, minor changes in bond distances. The results indicate that these changes are probably due to the decreased metal-ion size.

In addition, we have attempted to extend the normal "direct methods" by use of a new phase relationship called the "quadruple product". The method has been tried successfully on  $\text{Cs}_3\text{Sb}_2\text{Cl}_9$ .



STRUCTURE OF 2[TETRA(TRIMETHYLSILYL)CYCLOHEXENE-  
1-YL]HEPTAMETHYLTRISILANE

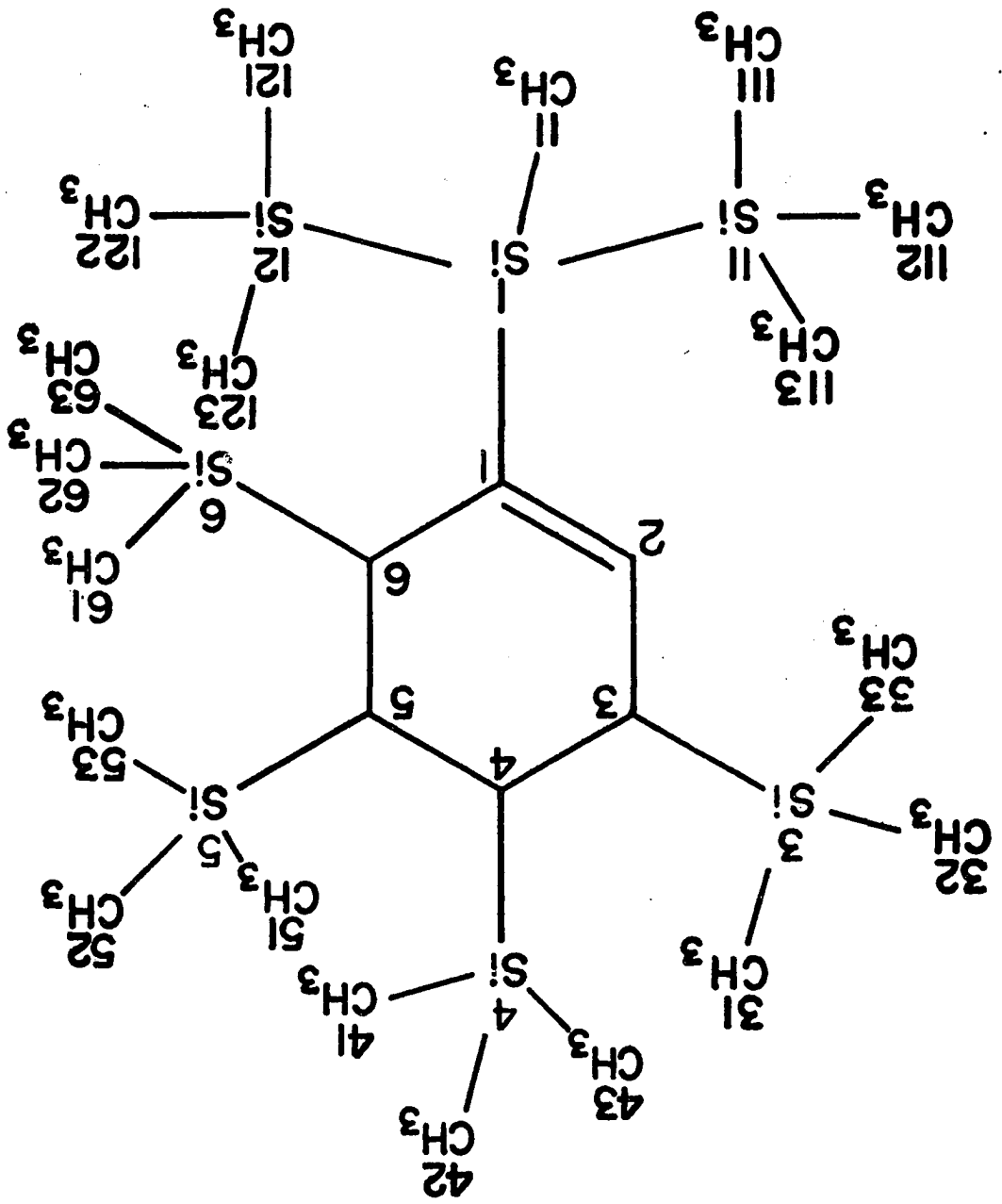
Introduction

Although the structures of inorganic silicon compounds as well as a number of organic siloxanes and silsesquioxanes have been studied extensively, relatively little structural information is available for organosilicon compounds which contain Si-Si bonds. Gas phase electron diffraction was used to investigate the structures of disilane<sup>1</sup> and hexamethyldisilane<sup>2</sup>, but the only compound of this type to be investigated by single-crystal X-ray diffraction techniques prior to the present study was bistetramethyldisilanilene-dioxide,  $((\text{CH}_3)_4\text{Si}_2\text{O})_2$ <sup>3</sup>. The title compound, 2-[tetra(trimethylsilyl)cyclohexene-1-yl]heptamethyltrisilane, hereafter referred to as TTCH, is of interest because of the trisilane moiety. The molecular configuration and the numbering scheme used in this investigation are seen in Figure 1. TTCH was obtained as the major product<sup>4</sup> in the reaction of phenylmethyldichlorosilane and chlorotrimethylsilane with metallic lithium in tetrahydrofuran, and was unambiguously characterized only after this structural investigation.

Experimental

A sample of TTCH, mp 121<sup>o</sup>, was kindly supplied by Professor Gilman of this department. After recrystallization

Figure 1. The molecular structure of TTCH (the ring carbons are numbered from 1 through 6 and the silicon atoms which are bonded to them have the same number as the carbon to which they are attached. Substituents on each silicon atom are identified by moving the silicon number one digit to the left)



from a 1:1 solution of methanol and ethyl acetate, many small, colorless crystals were obtained and were used without further purification. Weissenberg and precession photographs made with  $\text{CuK}\alpha$  and  $\text{MoK}\alpha$  radiation, respectively, indicated orthorhombic symmetry. Systematic absences observed for  $0k1$  reflections with  $k + l$  odd, and for  $h0l$  reflections with  $h$  odd, limited the choice of space groups to  $\text{Pna}2_1$  or  $\text{Pnma}$ . Accurate unit cell parameters were obtained from a least-squares refinement based on the  $2\theta$  values for 16 reflections which had been carefully measured on a General Electric diffractometer using  $\text{CrK}\alpha$  radiation. The  $\alpha_1$  and  $\alpha_2$  components were unresolved. Hence the wavelength used was the weighted mean of  $\alpha_1$  and  $\alpha_2$ ,  $\lambda = 2.291 \text{ \AA}$ . The unit cell parameters and their standard deviations based on the elements of the least-squares inverse matrix are  $a = 24.081 \pm 0.008$ ,  $b = 9.839 \pm 0.007$ ,  $c = 15.973 \pm 0.009 \text{ \AA}$ , and  $V = 3784 \text{ \AA}^3$ . The density as measured by flotation in a methanol-glycerol mixture was  $0.97 \text{ g/cm}^3$ ; the density calculated with  $Z = 4$  was  $0.98 \text{ g/cm}^3$ . A General Electric XRD-5 X-ray unit equipped with a single-crystal orienter and scintillation counter was used with  $\text{MoK}\alpha$  radiation ( $\lambda = 0.7107 \text{ \AA}$ ) in the moving-crystal-moving-counter mode ( $\theta$ ,  $2\theta$  coupling) to measure intensities. A 100-sec scan covering  $1.67^\circ$  in  $2\theta$  was used for each reflection. The take-off angle was  $1.0^\circ$ . Since the backgrounds were seen to be a function of  $\theta$  only,

the backgrounds for individual reflections were obtained from a plot of background versus  $2\theta$ . One crystallographically independent octant of data was measured within a  $2\theta$  sphere of  $45^\circ$  ( $\sin\theta/\lambda = 0.538$ ) beyond which no reflections were observed to have intensities significantly above the background. These data, after correction for noncharacteristic radiation streaks<sup>5</sup> and Lorentz-polarization factors, were reduced to structure factors. The crystal used for intensity measurements had approximate dimensions 0.2 x 0.2 x 0.4 mm. The minimum and maximum transmittances were 91% and 97% based on  $\mu = 2.50 \text{ cm}^{-1}$ . Consequently no absorption correction was made. In an attempt to account for systematic as well as random errors standard deviations were assigned to the intensity data according to the formula:

$$\sigma(I) = [C_T + C_B + C_S + (0.04C_T)^2 + (0.04C_B)^2 + (0.06C_S)^2]^{1/2}$$

where  $C_T$ ,  $C_B$ , and  $C_S$  are, respectively, the total counts, background counts, and streak counts. The quadratic terms correspond to estimated systematic errors of 4% in intensity and background measurements, and 6% in the streak correction. The estimated standard deviation for each structure factor was obtained by the method of finite differences<sup>5</sup>

$$\sigma(F) = ([I + \sigma(I)]^{1/2} - I^{1/2}) / (L_p)^{1/2}$$

where  $L_p$  is the Lorentz-polarization factor. Of the 1423

measured reflections, 198 had  $F < 3\sigma(F)$  and were excluded from the refinement.

Since the general multiplicity of the centrosymmetric space group, Pnma, is 8, four molecules of TTCH could occupy one unit cell in this space group only if each possessed either a center of symmetry or a mirror plane. The improbability of either symmetry in TTCH molecules indicated the noncentrosymmetric space group Pna2<sub>1</sub>. The successful solution of the structure verified this space group assignment. The Si atoms were located by the use of a three-dimensional, superposition procedure starting with a well resolved peak in the Harker section of the sharpened Patterson map (the thermal parameter, B, used for sharpening was  $2.0 \text{ \AA}^2$ ). In the resultant map, a center of symmetry relating two images was readily found. Utilizing one additional superposition and a knowledge of the space group symmetry, six of the seven Si atoms were located. Because of the large number of apparently equal peaks in the three-dimensional electron density map, the final silicon atom, Si<sub>5</sub>, could not be distinguished from the many, as yet unassigned, carbon peaks. A centrosymmetric projection of this Fourier map along the c-axis, however, clearly yielded the x and y coordinates of Si<sub>5</sub>. The z coordinate was readily obtained by searching the three-dimensional map along the line defined by x and y. Subsequent three-dimensional Fourier syntheses revealed

the locations of all of the carbon atoms. Calculations were performed on IBM/360 models 50 and 65 computers using a series of unpublished programs developed at Iowa State University, the Oak Ridge least-squares program<sup>6</sup>, and the block-diagonal least-squares program of the National Research Council of Canada<sup>7</sup>. Scattering factors for neutral silicon and carbon atoms were those of Hanson *et al.*<sup>8</sup>. Only the  $x$  and  $y$  parameters of  $\text{Si}_{11}$  were varied in the least-squares refinement in order to fix the origin of the polar unit cell. The full-matrix isotropic refinement converged to a conventional  $R$ ,  $R = \Sigma | |F_o| - |F_c| | / \Sigma |F_o|$ , of 0.116. The function minimized was  $\Sigma w (|F_o| - |F_c|)^2$  in which the weight,  $w$ , was  $1/\sigma^2(F)$ . The anisotropic refinement of 287 positional and temperature factors necessitated use of the block-diagonal approximation. In the final stages of refinement a modified weighting function was used in order to remove the dependence of  $\langle w (|F_o| - |F_c|)^2 \rangle$  on  $F_o$ . The modified weighting function was  $w = 1/(\sigma^2(F) + 0.005F^2)$ . Convergence was achieved with a conventional  $R$  factor of 0.07 and a weighted  $R$  factor,  $R_w = (\Sigma w (|F_o| - |F_c|)^2 / \Sigma w F_o^2)^{1/2}$ , of 0.10. The standard deviation of a reflection of unit weight was 1.009. A consideration of the isotropic and anisotropic  $R$  factors permits rejection at the 0.005 level of the hypothesis that all atoms vibrate isotropically<sup>9</sup>. A difference map was calculated in an attempt to determine the positions of the hydrogens. How-

ever, due to the large thermal vibrations in the molecule, the hydrogen atoms could not be located. Final positional and thermal parameters along with their estimated standard deviations are listed in Figure 2. The neglect of interatomic correlations in the block-diagonal approximation leads to underestimation of the standard deviations. Experience in this laboratory has shown that the block-diagonal standard deviations and quantities calculated from them should be multiplied by 1.2 for comparison with full-matrix values. Calculated structure factors are compared with the observed values in Figure 3.

#### Results and Discussion

The molecular structure of TTCH is shown in Figure 4 which was prepared by the computer utilizing Johnson's ORTEP program<sup>10</sup>. TTCH absorbs in the ultraviolet with a maximum at 241 m $\mu$ <sup>11</sup> whereas trisilanes usually absorb at 215 m $\mu$ <sup>12</sup>. Such a shift toward the visible is common in the spectra of silanes which have phenyl or vinyl substituents and has been explained in terms of p $\pi$ -d $\pi$  interactions with the unoccupied 3d orbitals on silicon<sup>13,14</sup>. Accordingly the carbon-carbon double bond in TTCH was placed vinylic to the trisilane moiety by Gilman et al.<sup>4</sup>. The carbon-carbon double bond of the cyclohexene system is unambiguously located between C<sub>1</sub> and C<sub>2</sub> on the basis of interatomic distances. Thus the structure proposed by Gilman et al.<sup>4</sup> is verified.



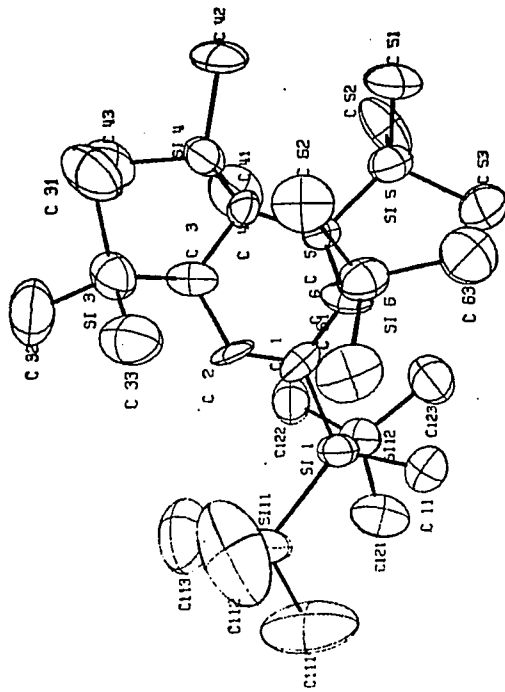
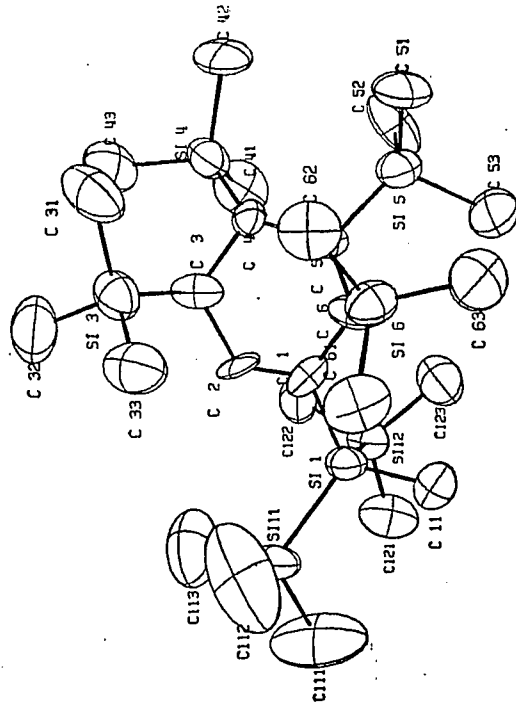
Figure 2. Fractional atomic coordinates and anisotropic temperature coefficients ( $10^4 \times \sigma$  is given in parentheses.  $B$ 's are times  $10^4$  and have the form  $\exp [-(h^2 \cdot B_{11} + k^2 \cdot B_{22} + l^2 \cdot B_{33} + \underline{kl} \cdot B_{23} + \underline{hl} \cdot B_{13} + \underline{hk} \cdot B_{12})]$ )

ATOM	X	Y	Z	$\beta_{11}$	$\beta_{22}$	$\beta_{33}$	$\beta_{23}$	$\beta_{13}$	$\beta_{12}$
SI 1	-0.0173(2)	0.4391(6)	0.3002(4)	14(1)	134(7)	60(3)	11(9)	-4(3)	4(4)
SI 11	-0.0854(2)	0.2947(6)	0.3541(-)	16(1)	157(8)	101(4)	-8(12)	9(4)	-14(5)
SI 12	-0.0302(2)	0.6653(5)	0.3455(5)	21(1)	114(7)	66(3)	-2(10)	1(4)	2(5)
SI 3	0.1297(2)	0.1504(6)	0.4857(4)	25(1)	124(7)	66(4)	27(10)	-12(4)	-8(5)
SI 4	0.2050(2)	0.5079(6)	0.5019(4)	19(1)	143(7)	62(3)	-31(10)	-15(4)	-3(5)
SI 5	0.2075(2)	0.6148(6)	0.2787(5)	17(1)	160(8)	74(4)	43(11)	10(1)	-4(5)
SI 6	0.1301(2)	0.2862(6)	0.2092(4)	18(1)	169(8)	58(3)	-32(10)	-1(4)	24(5)
C 1	0.0554(6)	0.3917(16)	0.3328(11)	18(3)	115(21)	37(9)	-39(26)	-18(9)	34(14)
C 2	0.0619(6)	0.3504(16)	0.4112(12)	6(3)	133(24)	59(11)	8(30)	-22(9)	21(14)
C 3	0.1180(6)	0.3369(18)	0.4571(13)	14(3)	147(25)	72(12)	-29(32)	-1(11)	-7(15)
C 4	0.1697(6)	0.4194(16)	0.4142(11)	17(3)	95(22)	50(10)	54(28)	-20(10)	-17(14)
C 5	0.1486(6)	0.5090(16)	0.3394(11)	13(3)	124(21)	43(9)	-11(28)	-6(9)	1(14)
C 6	0.1047(6)	0.4360(17)	0.2817(14)	10(3)	118(22)	81(13)	-18(34)	16(11)	16(14)
C 11	-0.0246(8)	0.4398(25)	0.1813(14)	27(5)	310(44)	56(13)	-62(42)	-16(13)	16(24)
C 31	0.2062(8)	0.1025(19)	0.4837(17)	32(5)	140(26)	116(18)	38(43)	-34(18)	13(19)
C 32	0.0999(11)	0.1218(27)	0.5892(17)	54(8)	236(40)	76(15)	94(45)	27(19)	14(30)
C 33	0.0934(8)	0.0335(20)	0.4144(19)	25(4)	142(29)	128(19)	28(42)	-4(15)	12(19)
C 41	0.1702(10)	0.6748(24)	0.5245(15)	41(6)	232(38)	76(16)	-68(42)	-11(16)	23(26)
C 42	0.2820(7)	0.5208(29)	0.4790(16)	12(3)	400(50)	87(15)	33(50)	-22(13)	-42(22)
C 43	0.1999(9)	0.4151(23)	0.6029(14)	30(5)	233(37)	65(13)	-19(39)	-29(14)	-2(23)
C 51	0.2652(7)	0.5210(24)	0.2431(16)	13(3)	277(39)	106(17)	56(45)	12(13)	14(19)
C 52	0.2235(10)	0.7722(22)	0.3355(17)	48(6)	165(32)	103(17)	29(44)	53(20)	-84(24)
C 53	0.1659(8)	0.6967(26)	0.1788(16)	24(5)	308(45)	87(17)	100(48)	-1(14)	51(25)
C 61	0.0714(9)	0.1635(22)	0.1803(16)	34(5)	193(35)	92(16)	-92(43)	-12(17)	16(22)
C 62	0.1873(9)	0.1820(19)	0.2461(15)	32(5)	130(26)	85(15)	-64(34)	2(14)	10(19)
C 63	0.1477(9)	0.3565(30)	0.1079(15)	29(5)	406(55)	58(14)	-36(49)	30(14)	68(28)
C 111	-0.1553(10)	0.3457(30)	0.3133(33)	27(5)	310(51)	297(48)	175(89)	-31(27)	-84(27)
C 112	-0.0673(17)	0.1144(30)	0.3257(29)	98(15)	224(46)	232(41)	175(75)	158(42)	-202(44)
C 113	-0.0856(13)	0.2938(37)	0.4675(20)	62(10)	459(73)	87(19)	-119(65)	41(25)	-97(45)
C 121	-0.1044(9)	0.7195(25)	0.3359(19)	33(5)	237(39)	117(19)	48(48)	4(19)	37(25)
C 122	-0.0065(9)	0.6859(23)	0.4564(14)	38(6)	217(35)	59(12)	-62(37)	-16(19)	44(24)
C 123	0.0147(9)	0.7800(23)	0.2772(17)	31(5)	206(34)	93(19)	68(43)	19(17)	27(23)

Figure 3. Observed and calculated structure factors (each group of data contains, going from left to right,  $h$ ,  $l$ ,  $\underline{F}_O$ ,  $w$ ,  $\underline{F}_C$  while the data are headed by the value of  $k$ . Structure factors are in electrons times 10. A negative  $\underline{F}_O$  indicates a reflection which is considered unobserved)



Figure 4. Stereoscopic representation of TTCH (anisotropic thermal vibration is indicated by 50% probability ellipsoids)



The bond distances and angles in TTCH are listed in Table 1. Anisotropic thermal vibration is indicated in Figure 4 by the ellipsoids which are drawn to a scale such that the atomic centers are found within them 50% of the time. Root-mean-square amplitudes of thermal vibration along the principal axes 1-3 of the ellipsoids are presented in Table 2. There are 23 crystallographically independent Si-C(sp<sup>3</sup>) bonds in TTCH all of which should be chemically equivalent. However, a rather large scatter is observed in these Si-C bond lengths (1.81 - 1.97 Å). Such a range is not uncommon in organosilicon compounds<sup>3,15</sup> and, in the case of the methyl-carbon to silicon distances, can be attributed to the large amplitudes of thermal motion and methyl-methyl group steric interactions. The ring-carbon atoms to silicon atom distances are in much better agreement (1.86 - 1.91 Å) with exception of the Si<sub>6</sub>-C<sub>6</sub> distance of 1.97(2) Å which is apparently lengthened due to steric interactions with the adjacent trisilane moiety. In addition, the inability to silylate the last ring-carbon atom can be attributed to this effect in agreement with mechanisms proposed by Harrell<sup>11</sup> and Weyenberg and Toporger.<sup>16</sup> The mean Si-Si distance is  $2.35 \pm 0.01$  Å which is in agreement with the value of  $2.3517 \pm 0.0001$  Å in metallic silicon.<sup>17</sup> With respect to the approximate plane of the ring, the four trimethylsilyl groups are bonded  $\delta$ ,  $\alpha$ ,  $\beta$ ,  $\beta$ , to ring carbons C<sub>3</sub>, C<sub>4</sub>, C<sub>5</sub>,

Table 1. Distances ( $\text{\AA}$ ) and angles (deg) with standard deviations in parentheses

Bond	Value	Angle	Value	Angle	Value
Non-methyl bond distances and angles					
Si <sub>1</sub> -Si <sub>11</sub>	2.335(7)	Si <sub>11</sub> -Si <sub>1</sub> -Si <sub>12</sub>	111.6(0.2)	Si <sub>4</sub> -C <sub>4</sub> -C <sub>3</sub>	105.4(0.9)
Si <sub>1</sub> -Si <sub>12</sub>	2.361(8)	Si <sub>11</sub> -Si <sub>1</sub> -C <sub>1</sub>	115.6(0.5)	Si <sub>4</sub> -C <sub>4</sub> -C <sub>5</sub>	117.3(0.9)
Si <sub>1</sub> -C <sub>1</sub>	1.884(17)	Si <sub>12</sub> -Si <sub>1</sub> -C <sub>1</sub>	105.7(0.5)	C <sub>3</sub> -C <sub>4</sub> -C <sub>5</sub>	110.6(1.2)
Si <sub>3</sub> -C <sub>3</sub>	1.912(19)	Si <sub>1</sub> -C <sub>1</sub> -C <sub>2</sub>	116.5(1.0)	Si <sub>5</sub> -C <sub>5</sub> -C <sub>4</sub>	119.1(0.9)
Si <sub>4</sub> -C <sub>4</sub>	1.856(17)	Si <sub>1</sub> -C <sub>1</sub> -C <sub>6</sub>	120.7(1.0)	Si <sub>5</sub> -C <sub>5</sub> -C <sub>6</sub>	113.2(0.9)
Si <sub>5</sub> -C <sub>5</sub>	1.893(17)	C <sub>6</sub> -C <sub>1</sub> -C <sub>2</sub>	120.4(1.3)	C <sub>5</sub> -C <sub>5</sub> -C <sub>6</sub>	113.9(1.6)
Si <sub>6</sub> -C <sub>6</sub>	1.971(18)	C <sub>1</sub> -C <sub>2</sub> -C <sub>3</sub>	125.4(1.3)	Si <sub>6</sub> -C <sub>6</sub> -C <sub>5</sub>	118.4(0.9)
C <sub>1</sub> -C <sub>2</sub>	1.325(22)	Si <sub>3</sub> -C <sub>3</sub> -C <sub>4</sub>	117.7(1.0)	Si <sub>6</sub> -C <sub>6</sub> -C <sub>1</sub>	110.3(0.9)
C <sub>2</sub> -C <sub>3</sub>	1.544(24)	Si <sub>3</sub> -C <sub>3</sub> -C <sub>2</sub>	107.3(1.0)	C <sub>5</sub> -C <sub>6</sub> -C <sub>1</sub>	110.1(1.2)
C <sub>3</sub> -C <sub>4</sub>	1.635(24)	C <sub>2</sub> -C <sub>3</sub> -C <sub>4</sub>	115.1(1.2)		
C <sub>4</sub> -C <sub>5</sub>	1.569(23)				
C <sub>5</sub> -C <sub>6</sub>	1.577(23)				
C <sub>6</sub> -C <sub>1</sub>	1.504(24)				



Table 1. (Continued)

Bond	Value	Bond	Value	Bond	Value
Bond distances involving methyl groups					
Si <sub>1</sub> -C <sub>11</sub>	1.908(23)	Si <sub>4</sub> -C <sub>43</sub>	1.857(23)	Si <sub>6</sub> -C <sub>63</sub>	1.911(25)
Si <sub>3</sub> -C <sub>31</sub>	1.903(23)	Si <sub>5</sub> -C <sub>51</sub>	1.899(23)	Si <sub>11</sub> -C <sub>111</sub>	1.873(35)
Si <sub>3</sub> -C <sub>32</sub>	1.824(27)	Si <sub>5</sub> -C <sub>52</sub>	1.878(25)	Si <sub>11</sub> -C <sub>112</sub>	1.882(39)
Si <sub>3</sub> -C <sub>33</sub>	1.840(24)	Si <sub>5</sub> -C <sub>53</sub>	1.971(24)	Si <sub>11</sub> -C <sub>113</sub>	1.811(33)
Si <sub>4</sub> -C <sub>41</sub>	1.878(25)	Si <sub>6</sub> -C <sub>61</sub>	1.889(24)	Si <sub>12</sub> -C <sub>121</sub>	1.873(27)
Si <sub>4</sub> -C <sub>42</sub>	1.895(24)	Si <sub>6</sub> -C <sub>62</sub>	1.814(24)	Si <sub>12</sub> -C <sub>122</sub>	1.871(23)
				Si <sub>12</sub> -C <sub>123</sub>	1.906(23)

Table 1. (Continued)

Angle	Value	Angle	Value	Angle	Value
Bond angles involving methyl groups					
C <sub>11</sub> -Si <sub>1</sub> -C <sub>1</sub>	112.0(0.9)	C <sub>41</sub> -Si <sub>4</sub> -C <sub>43</sub>	103.6(1.0)	C <sub>62</sub> -Si <sub>6</sub> -C <sub>63</sub>	109.3(1.0)
C <sub>11</sub> -Si <sub>1</sub> -Si <sub>11</sub>	107.7(0.7)	C <sub>42</sub> -Si <sub>4</sub> -C <sub>43</sub>	105.4(1.0)	Si <sub>1</sub> -Si <sub>12</sub> -C <sub>121</sub>	111.7(0.8)
C <sub>11</sub> -Si <sub>1</sub> -Si <sub>12</sub>	106.8(0.7)	C <sub>5</sub> -Si <sub>5</sub> -C <sub>51</sub>	115.3(0.9)	Si <sub>1</sub> -Si <sub>12</sub> -C <sub>122</sub>	110.6(0.7)
C <sub>3</sub> -Si <sub>3</sub> -C <sub>31</sub>	112.1(0.9)	C <sub>5</sub> -Si <sub>5</sub> -C <sub>52</sub>	113.6(0.9)	Si <sub>1</sub> -Si <sub>12</sub> -C <sub>123</sub>	107.9(0.7)
C <sub>3</sub> -Si <sub>3</sub> -C <sub>32</sub>	107.9(1.0)	C <sub>5</sub> -Si <sub>5</sub> -C <sub>53</sub>	111.2(0.9)	C <sub>121</sub> -Si <sub>12</sub> -C <sub>122</sub>	109.7(1.1)
C <sub>3</sub> -Si <sub>3</sub> -C <sub>33</sub>	112.4(0.9)	C <sub>51</sub> -Si <sub>5</sub> -C <sub>52</sub>	107.7(1.0)	C <sub>122</sub> -Si <sub>12</sub> -C <sub>123</sub>	107.8(1.0)
C <sub>31</sub> -Si <sub>3</sub> -C <sub>32</sub>	111.0(1.1)	C <sub>51</sub> -Si <sub>5</sub> -C <sub>53</sub>	107.6(1.0)	C <sub>121</sub> -Si <sub>12</sub> -C <sub>123</sub>	109.0(1.1)
C <sub>31</sub> -Si <sub>3</sub> -C <sub>33</sub>	107.2(1.0)	C <sub>52</sub> -Si <sub>5</sub> -C <sub>53</sub>	100.3(1.0)	Si <sub>1</sub> -Si <sub>11</sub> -C <sub>111</sub>	109.9(1.1)
C <sub>32</sub> -Si <sub>3</sub> -C <sub>33</sub>	106.1(1.0)	C <sub>6</sub> -Si <sub>6</sub> -C <sub>61</sub>	110.4(0.9)	Si <sub>1</sub> -Si <sub>11</sub> -C <sub>112</sub>	108.8(1.2)
C <sub>4</sub> -Si <sub>4</sub> -C <sub>41</sub>	110.6(0.9)	C <sub>6</sub> -Si <sub>6</sub> -C <sub>62</sub>	117.9(0.9)	Si <sub>1</sub> -Si <sub>11</sub> -C <sub>113</sub>	111.9(1.0)
C <sub>4</sub> -Si <sub>4</sub> -C <sub>42</sub>	109.5(0.9)	C <sub>6</sub> -Si <sub>6</sub> -C <sub>63</sub>	109.3(0.9)	C <sub>111</sub> -Si <sub>11</sub> -C <sub>112</sub>	112.1(1.6)
C <sub>4</sub> -Si <sub>4</sub> -C <sub>43</sub>	113.3(0.9)	C <sub>61</sub> -Si <sub>6</sub> -C <sub>62</sub>	105.3(1.0)	C <sub>111</sub> -Si <sub>11</sub> -C <sub>113</sub>	110.3(1.5)
C <sub>41</sub> -Si <sub>4</sub> -C <sub>42</sub>	114.5(1.1)	C <sub>61</sub> -Si <sub>6</sub> -C <sub>63</sub>	103.7(1.0)	C <sub>112</sub> -Si <sub>11</sub> -C <sub>113</sub>	103.7(1.6)

Table 2. Root-mean-square amplitude of vibration (angstroms x 10<sup>3</sup>)

Atom	Min.	Med.	Max.	Atom	Min.	Med.	Max.
Si <sub>1</sub>	200	252	282	C <sub>33</sub>	250	280	406
Si <sub>11</sub>	207	280	362	C <sub>41</sub>	277	330	382
Si <sub>12</sub>	235	250	291	C <sub>42</sub>	160	335	450
Si <sub>3</sub>	238	255	310	C <sub>43</sub>	237	331	344
Si <sub>4</sub>	216	259	302	C <sub>51</sub>	191	337	399
Si <sub>5</sub>	216	265	327	C <sub>52</sub>	200	340	445
Si <sub>6</sub>	218	262	310	C <sub>53</sub>	238	310	426
C <sub>1</sub>	178	190	297	C <sub>61</sub>	260	311	386
C <sub>2</sub>	94	261	289	C <sub>62</sub>	227	308	348
C <sub>3</sub>	200	259	312	C <sub>63</sub>	204	324	461
C <sub>4</sub>	178	198	301	C <sub>111</sub>	229	390	637
C <sub>5</sub>	188	231	252	C <sub>112</sub>	218	393	703
C <sub>6</sub>	155	246	328	C <sub>113</sub>	300	377	535
C <sub>11</sub>	240	292	401	C <sub>121</sub>	285	347	402
C <sub>31</sub>	241	293	407	C <sub>122</sub>	248	293	383
C <sub>32</sub>	256	359	421	C <sub>123</sub>	281	288	386

and C<sub>6</sub>, respectively. The torsion angles about the three C(sp<sup>3</sup>)-C(sp<sup>3</sup>) bonds within the cyclohexene ring are listed in Table 3. Methyl groups on adjacent silyl groups are meshed as follows: C<sub>11</sub> is between C<sub>61</sub> and C<sub>63</sub>; C<sub>51</sub>, between C<sub>62</sub> and C<sub>63</sub>; C<sub>52</sub>, between C<sub>41</sub> and C<sub>42</sub>; and C<sub>43</sub>, between C<sub>31</sub> and C<sub>32</sub>. In this way intramolecular nonbonded repulsions are minimized. TTCH is obviously a racemate as is required by the presence of improper symmetry elements in the space group. The molecular packing is apparently governed entirely by steric factors because there exists no possibility for hydrogen bonding. The shortest intermolecular distances were 3.86 Å between C<sub>11</sub> and C<sub>122</sub> (molecule at  $\bar{x}$ ,  $\bar{y}$ , 1/2 + z) and 3.88 Å between C<sub>53</sub> and C<sub>113</sub> (molecule at  $\bar{x}$ ,  $\bar{y}$ , 1/2 + z).

Table 3. Torsion angles

Bond	Torsion angle (degrees)
C <sub>3</sub> - C <sub>4</sub>	84.8
C <sub>4</sub> - C <sub>5</sub>	59.3
C <sub>5</sub> - C <sub>6</sub>	69.5

STRUCTURE OF *cis*-  
DICHLOROBIS(DIMETHYLPHENYLPHOSPHINE)PALLADIUM(II)

Introduction

It has been observed that square planar complexes of the type  $\text{PdX}_2\text{Y}_2$ , where X is a halide, very often adopt the trans configuration.<sup>18</sup> In fact, only recently have any cis complexes of this type been characterized. The cis, chloro complexes usually form pale yellow or colorless crystals while crystals of the trans complexes are more decidedly yellow.<sup>19</sup> However, a recent far-infrared study<sup>20</sup> by R. Keiter of  $\text{PdCl}_2(\text{P}(\text{CH}_3)_2\text{C}_6\text{H}_5)_2$  which forms distinctly yellow crystals, indicated that this compound unlike  $\text{PdI}_2(\text{P}(\text{CH}_3)_2\text{C}_6\text{H}_5)_2$ <sup>21</sup> was probably not trans but no configuration could be assigned from the spectra. Therefore we undertook a crystal structure investigation to determine if the complex is square-planar and, if so, which isomer is present.

Experimental

A sample of this compound was kindly supplied by R. Keiter and the yellow crystals were used without further purification. Inspection of the crystals showed them to be square plates with sharply-defined faces. Weissenberg and precession photographs indicated a tetragonal space group with systematic extinctions of the type  $00\bar{1}, \bar{1} = 2n + 1$ ;  $hk0, h + k = 2n + 1$ . These conditions indicate the space

group to be  $P4_2/n$ . In addition, systematically weak reflections of the type  $\underline{h} + \underline{k} = 2n + 1$  and  $\underline{l} = 2n + 1$  for general  $\underline{hkl}$  reflections were observed.

The unit cell dimensions were determined by least-squares fit of 13 independent reflections whose  $2\theta$  values were determined from Weissenberg photographs calibrated with Al powder lines. The values obtained were  $\underline{a} = \underline{b} = 9.324 \pm 0.004 \overset{\circ}{\text{Å}}$  and  $\underline{c} = 21.485 \pm 0.004 \overset{\circ}{\text{Å}}$ . The measured density was 1.61 g/cc obtained by flotation techniques in a solution of diiodomethane and 1-bromopropane. The calculated density with four molecules per unit cell ( $V_c = 1868 \overset{\circ}{\text{Å}}^3$ ) is 1.62 g/cc.

A crystal of approximate dimensions 0.2 x 0.2 x 0.1 mm was selected for use in data collection. The crystal was mounted such that the (110) axis would be coincident with the phi axis of the diffractometer. Data were collected at room temperature using a Hilger-Watts four circle diffractometer equipped with a scintillation counter employing Zr-filtered Mo-K $\alpha$  ( $\lambda = 0.7107 \overset{\circ}{\text{Å}}$ ) radiation. All data within a  $2\theta$  sphere of 60 deg ( $\sin\theta/\lambda = 0.70$ ) were measured using a  $\theta$ - $2\theta$  coupled scan with a five deg take-off angle. Stationary-counter measurements of the background were made at the beginning and the end of each scan. The scan range was over 50 steps of 0.01 deg, one step per 0.4096 sec, and was increased by 1 step per deg increase in  $2\theta$  to insure complete integration over the entire peak. The length of the back-

ground measurement was adjusted accordingly. No appreciable decrease in the intensities of three standard reflections which were measured periodically throughout the data taking period was observed.

The measured intensities were corrected for background, Lorentz and polarization effects, and for adsorption<sup>7</sup> ( $\mu = 14.2 \text{ cm}^{-1}$ ); minimum and maximum transmission factors were 0.67 and 0.87, respectively. The standard deviations were assigned to the intensities according to the following formula:

$$\sigma(I) = (C_t + C_b + (0.05 C_t)^2 + (0.10 C_b)^2 + (0.05 C_n)^2)^{1/2}$$

where  $C_t$ ,  $C_b$ ,  $C_n$  and  $A$  are the total counts, background counts, net counts, and the absorption factor. The quadratic terms correspond to the estimated systematic errors in the intensity, background and absorption correction of 5, 10 and 5% respectively. The standard deviations in the structural amplitudes were obtained by the method of finite differences<sup>5</sup>,

$$\sigma(F_o) = ((I + \sigma(I))^{1/2} - I^{1/2}) / (Lp)^{1/2}$$

where  $Lp$  is the Lorentz-polarization factor. Of the 2877 measured reflections, 850 were found to have values of  $F_o$  less than  $2.0 \times \sigma(F_o)$ . These reflections were considered

to be unobserved and were not included in the refinement.

### Solution and Refinement of the Structure

Since the space group  $P4_2/n$  has eightfold general positions, it was necessary to place the palladium atoms in special positions. From a consideration of the systematically weak reflections of the type  $l = 2n + 1$ , the palladiums were placed in the fourfold special position denoted by the Wyckoff symbol 'e'; that is on the twofold axis perpendicular to the  $ab$  plane. Analysis of the Patterson map confirmed this supposition and allowed ready determination of the  $z$ -coordinate of the palladium. Three possible sets of chlorine and phosphorus positions were present due to pseudo mirroring. The correct set was determined by trial and error. These atoms gave a value of the discrepancy factor,  $R = \frac{\sum ||F_o| - |F_c||}{\sum |F_o|}$ , of 28% for a structure factor calculation with the heavy atoms alone. The remaining carbon atoms were located from a three-dimensional electron density map. The structure was refined isotropically to an  $R = 15.4\%$  using a modified version of ORFLS<sup>6,8,22</sup> and unit weights. At this point weights were changed to those based on individual statistics of the reflection ( $w = 1/\sigma(F_o)^2$ ). The ring hydrogen atoms were added in calculated positions assuming 1.0 Å for the C-H distance. No attempt was made to refine hydrogen positions. A final statistical analysis of the  $F_o$  and  $F_c$  values indicated a dependence on the scattering angle. The



relative weights were adjusted to remove this dependence. An additional 134 reflections were removed from the refinement because they failed to fulfill one of the following criteria:

$$||\underline{F}_O| - |\underline{F}_c|| < 10 \times \sigma(\underline{F}_O), \quad \left| \frac{\underline{F}_O}{\underline{F}_c} \right| < 5.0 \text{ or } \left| \frac{\underline{F}_c}{\underline{F}_O} \right| < 5.0.$$

The structure was refined anisotropically to a final R = 8.8% and a final weighted discrepancy index,  $R = (\sum w(\underline{F}_O - \underline{F}_c)^2)^{1/2} / (\sum w \underline{F}_O^2)^{1/2}$ , of 7.9%. Convergence was assumed when no parameter shift was greater than 0.1 of that parameter's estimated-standard deviation. A final difference electron density map showed no residual electron density above 1.4  $e^{-}/\text{\AA}^3$ .

In Figure 5 are the final values of the positional and thermal parameters and their respective estimated standard deviations.<sup>23</sup> Estimated standard deviations were derived from the inverse matrix. In Table 4 are given the root-mean-square amplitudes of vibration while in Figure 6 are listed the values of the observed and calculated structure factors on an absolute scale. The configuration of the molecule along with the numbering scheme used is shown in Figure 7.<sup>11</sup> Selected intramolecular distances and angles are given in Table 5 (see also Figure 8).

Figure 5. Fractional atomic coordinates and thermal parameters (estimated standard deviation are given in parentheses right adjusted to the least significant figure of the preceding number.  $\beta$ 's are times  $10^4$  and have the form  $\exp[-(\beta_{11}h^2 + \beta_{22}k^2 + \beta_{33}l^2 + \beta_{12}hk + \beta_{13}hl + \beta_{23}kl)]$ .)

ATOM	X	Y	Z	$\beta_{11}$	$\beta_{22}$	$\beta_{33}$	$\beta_{12}$	$\beta_{13}$	$\beta_{23}$
PD	0.75000	0.25000	0.25309(3)	69(1)	79(1)	12(0)	-1(1)	0	0
P	0.8863(2)	0.3716(2)	0.3222(1)	66(2)	74(2)	16(0)	-12(2)	2(1)	-2(1)
CL	0.8977(2)	0.3462(2)	0.1742(1)	151(3)	145(3)	17(0)	-26(2)	17(1)	2(1)
C 1	0.8162(7)	0.4163(7)	0.3973(3)	79(8)	79(8)	17(2)	-21(7)	0(3)	-5(3)
C 2	0.702(1)	0.511(1)	0.4011(4)	122(12)	164(14)	25(2)	6(10)	3(4)	-10(5)
C 3	0.650(1)	0.556(1)	0.4583(6)	159(15)	186(16)	35(3)	27(12)	22(6)	-21(6)
C 4	0.712(1)	0.513(1)	0.5114(5)	185(18)	287(23)	20(2)	-67(17)	19(6)	-38(6)
C 5	0.823(1)	0.417(1)	0.5103(4)	212(18)	239(20)	15(2)	-87(16)	-13(5)	11(5)
C 6	0.8759(9)	0.3678(9)	0.4527(4)	113(11)	165(13)	18(2)	-43(10)	-11(4)	6(4)
C 7	0.933(1)	0.5498(9)	0.2942(4)	187(15)	107(11)	22(2)	-75(10)	4(5)	7(4)
C 8	0.4411(8)	0.2143(9)	0.3340(4)	74(9)	170(14)	37(3)	35(9)	17(4)	16(5)
H 2	0.655	0.544	0.360	5.0					
H 3	0.570	0.631	0.463	5.0					
H 4	0.668	0.550	0.552	5.0					
H 5	0.872	0.382	0.550	5.0					
H 6	0.964	0.301	0.453	5.0					

Table 4. Root-mean-square amplitude of vibration ( $\text{\AA} \times 10^3$ )

Atom	Min.	Intermed.	Max.
Pd	169	174	187
P	158	185	199
C1	175	245	284
C <sub>1</sub>	157	196	215
C <sub>2</sub>	224	240	279
C <sub>3</sub>	202	296	324
C <sub>4</sub>	176	259	397
C <sub>5</sub>	179	246	376
C <sub>6</sub>	180	215	294
C <sub>7</sub>	158	234	320
C <sub>8</sub>	160	251	325

Figure 6. Observed and calculated structure amplitudes  
(in electrons x 10) for  $\text{PdCl}_2(\text{P}(\text{CH}_3)_2\text{C}_6\text{H}_5)_2$



Figure 7. A perspective drawing of cis-dichlorobis(dimethylphenylphosphine) palladium(II). Anisotropic thermal vibration is indicated by 50% probability ellipsoids

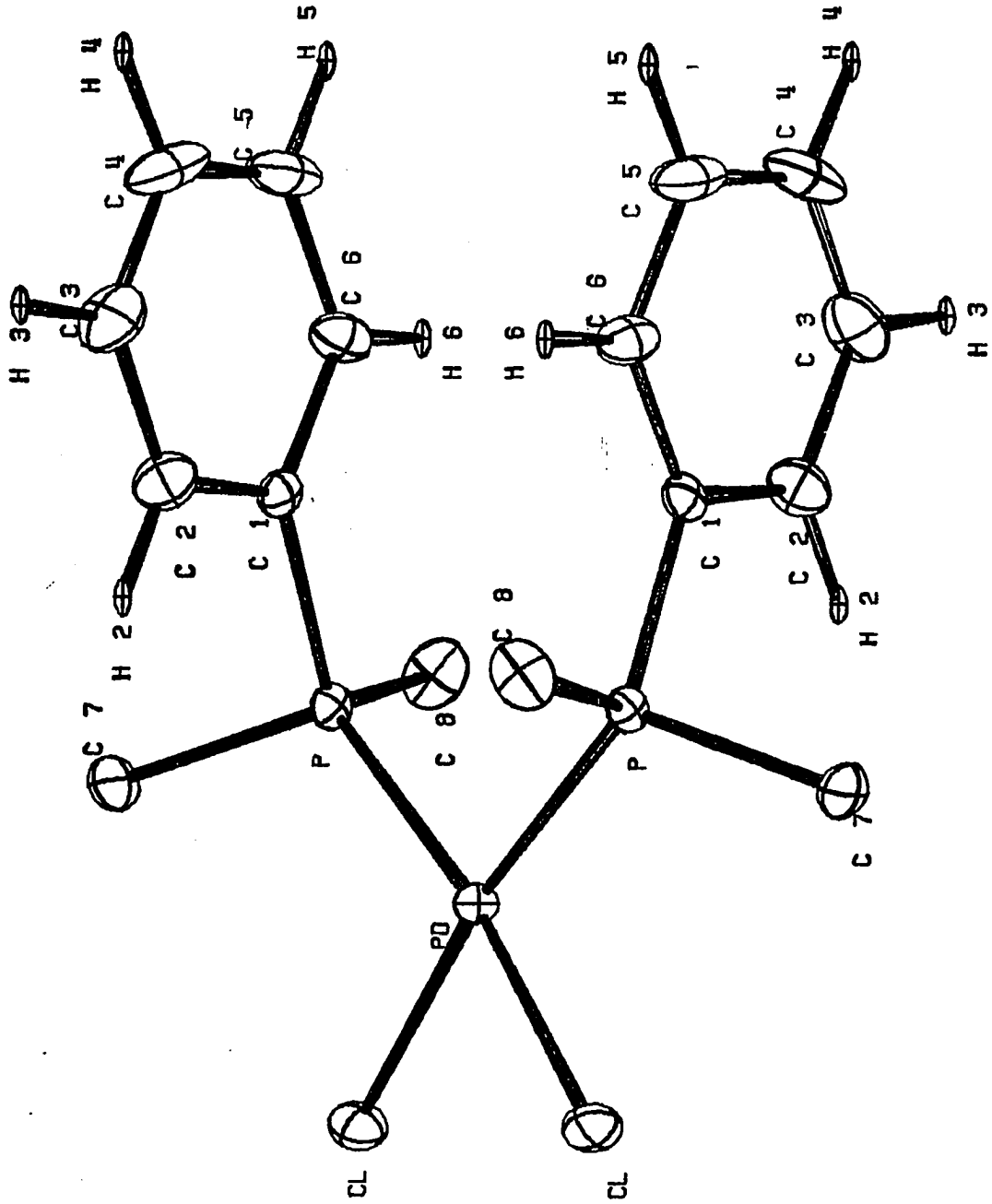
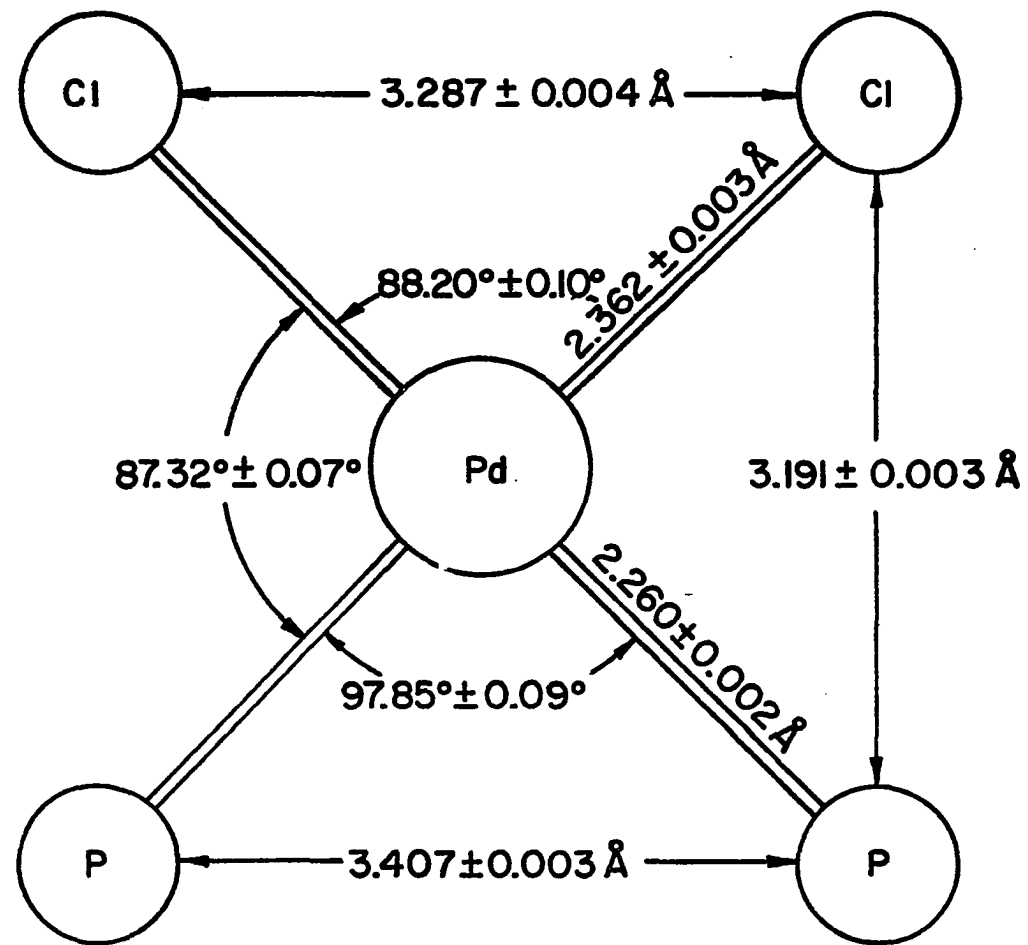




Table 5. Selected distances ( $\overset{\circ}{\text{\AA}}$ ) and angles (deg) with standard deviations in parentheses

Bond	Value	Angle	Value	Angle	Value
P-C1	3.191(3)	Cl-Pd-Cl'	88.2(1)	P-C <sub>1</sub> -C <sub>2</sub>	118.8(6)
P-P'	3.407(3)	Cl-Pd-P	87.32(7)	P-C <sub>1</sub> -C <sub>6</sub>	123.4(5)
Cl-Cl'	3.287(4)	P-Pd-P'	97.85(9)	P-C <sub>1</sub> -C <sub>4</sub>	174.6(5)
P-C <sub>1</sub>	1.791(7)	Pd-P-C <sub>1</sub>	120.2(2)	C <sub>6</sub> -C <sub>1</sub> -C <sub>2</sub>	117.7(7)
P-C <sub>7</sub>	1.819(7)	Pd-P-C <sub>7</sub>	112.0(3)	C <sub>1</sub> -C <sub>2</sub> -C <sub>3</sub>	121.0(8)
P-C <sub>8</sub>	1.815(8)	Pd-P-C <sub>8</sub>	111.7(3)	C <sub>2</sub> -C <sub>3</sub> -C <sub>4</sub>	120.6(9)
C <sub>1</sub> -C <sub>2</sub>	1.38(1)	C <sub>1</sub> -P-C <sub>7</sub>	100.0(3)	C <sub>3</sub> -C <sub>4</sub> -C <sub>5</sub>	120.6(9)
C <sub>2</sub> -C <sub>3</sub>	1.39(1)	C <sub>1</sub> -P-C <sub>8</sub>	107.4(4)	C <sub>4</sub> -C <sub>5</sub> -C <sub>6</sub>	119.4(8)
C <sub>3</sub> -C <sub>4</sub>	1.34(2)	C <sub>7</sub> -P-C <sub>8</sub>	103.8(6)	C <sub>5</sub> -C <sub>6</sub> -C <sub>1</sub>	120.6(8)
C <sub>4</sub> -C <sub>5</sub>	1.37(2)				
C <sub>5</sub> -C <sub>6</sub>	1.41(2)				
C <sub>6</sub> -C <sub>1</sub>	1.39(1)				

Figure 8. The arrangement of palladium and its four neighbors along with  
cogent distances and angles



## Description of the Structure

The complex is best described as approximately cis, square-planar. However there are slight, but significant distortions since the  $\angle$  Cl-Pd-Cl' ("'" denotes atom at  $\bar{x}$ ,  $\bar{y}$ ,  $\bar{z}$ ) has closed two deg and the  $\angle$  P-Pd-P' has opened some eight deg from their theoretical value of 90 deg. The Cl's are  $+0.13 \overset{\circ}{\text{Å}}$  and  $-0.13 \overset{\circ}{\text{Å}}$  from the least-squares plane defined by the palladium and its four nearest neighbors while the P's are  $\pm 0.12 \overset{\circ}{\text{Å}}$  from the plane. This is best viewed as a tetragonal distortion of 4.3 deg. The dihedral angle between the planes defined by the two phosphorus atoms and the palladium, and the two chlorine atoms and the palladium is  $171.3 \pm 0.1$  deg. The equations of the two planes in the form  $ax + by + cz - d = 0$  are ( $a = -0.66$ ,  $b = 0.746$ ,  $c = 0.00$ ,  $d = -2.92$ ) and ( $a = -0.546$ ,  $b = 0.838$ ,  $c = 0.00$ ,  $d = -1.86$ ), respectively.

The six carbon atoms in the phenyl ring showed no significant deviations from the best least-squares plane ( $a = 0.642$ ,  $b = 0.766$ ,  $c = -0.025$ ,  $d = 7.64$ ). The largest deviation from the plane was  $0.02 \overset{\circ}{\text{Å}}$  by  $C_4$  which is not statistically significant. The angles within the ring are all within three e.s.d.'s of the normal value of 120 deg. The ring bond distances also agree well with the expected value<sup>24</sup> of  $1.41 \overset{\circ}{\text{Å}}$  with the exception of the  $C_3-C_4$  distance which is slightly short.

## Discussion

The apparent deviations in this complex from the ideal square-planar configuration can be primarily attributed to overcrowding caused by the bulky phosphorus ligands cis to each other. The phenyl rings of the different phosphorus ligands on the same palladium interact sterically with one another. This accounts for the fact that the P-Pd-P' angle is 98 deg and the Pd-P-C<sub>1</sub> angle is found to be 120 deg since in this way steric interactions can be reduced. However, the two rings still approach each other within 3.2 Å, (C<sub>6</sub>-C'<sub>6</sub>); somewhat less than the sum of the van der Waals radii.<sup>24</sup> This interaction could also easily explain the slight screwing of the phenyl rings as indicated by the ∠ P-C<sub>1</sub>-C<sub>4</sub> of 174.6 deg. In order to accommodate the bulky phosphorus ligands, the chlorine atoms are forced closer together as shown by the ∠ Cl-Pd-Cl' of 88.2 deg. The Cl-Cl' distance of 3.287 Å is still greater than the distance of 2.88 Å which is the sum of the van der Waals radii of two chlorine atoms bonded to a common atom.<sup>25</sup> The slight tetragonal distortion may also be attributed to this overcrowding.

The agreement between the three nonequivalent P-C distances is good. The two phosphorus-methyl distances (1.819, 1.815 Å) are similar while the phosphorus-ring distance (1.791 Å) is just slightly shorter as would be expected from the slightly smaller covalent radii for the

ring carbon. The C-C distances are within 3% of their normal values and the Pd-Pd distance of  $6.6 \overset{\circ}{\text{Å}}$  is so great that any interaction is precluded despite an apparent alignment of the atoms.

The Pd-P bond in this compound ( $2.260 \pm 0.003 \overset{\circ}{\text{Å}}$ ) is significantly shorter than that found by Bailey and Mason<sup>21</sup> of  $2.333 \pm 0.007 \overset{\circ}{\text{Å}}$  in the trans-iodo complex, while the Cl-Pd bond ( $2.362 \pm 0.003 \overset{\circ}{\text{Å}}$ ) is significantly longer than that found by Bennett, Cotton and Weaver<sup>26</sup> of  $2.290 \pm 0.002 \overset{\circ}{\text{Å}}$  in  $\text{PdCl}_2(\text{DMSO})_2$ . The predicted values from the sum of the covalent radii are  $2.38 \overset{\circ}{\text{Å}}$  and  $2.28 \overset{\circ}{\text{Å}}$  for the Pd-P and Pd-Cl distances, respectively. Our results generally agree with those expected from a strong "trans-effect".<sup>27</sup> That is, the bond trans to a strongly "trans-direction" ligand such as phosphorus is weaker and therefore longer than a bond trans to the somewhat less "trans-directing" chlorine. As has already been noted by Messmer, Amma and Ibers,<sup>28</sup> these distances may be sensitive to the substituents on the phosphorus as well as variations in the halide used. However, it would be expected that as long as the ligands are similar with respect to their "trans-directing" ability, the effect on either the M-Cl or M-P distance would be the same whether M is Pd or Pt. In Table 6 are listed a number of M-Cl and M-P bond lengths involving ligands of similar "trans-directing" ability.<sup>29</sup> As would be expected from the different covalent radii and electro-negativities of palladium and platinum,

Table 6. Selected metal-phosphorus and metal chloride bond lengths

---

<u>Pd trans</u>			
Bond	Distance ( $\overset{\circ}{\text{A}}$ )	Compound	Ref.
Pd-P	2.333 $\pm$ 0.007	$\text{PdI}_2(\text{P}(\text{CH}_3)_2\text{C}_6\text{H}_5)_2$	21
Pd-Cl	2.287 $\pm$ 0.002	$\text{PdCl}_2(\text{DMSO})_2$	26
<u>Pd cis</u>			
Bond	Distance ( $\overset{\circ}{\text{A}}$ )	Compound	Ref.
Pd-P	2.260 $\pm$ 0.003	$\text{PdCl}_2(\text{P}(\text{CH}_3)_2\text{C}_6\text{H}_5)_2$	this work
Pd-Cl	2.362 $\pm$ 0.003	"	"
$\Delta$ <u>trans</u> to <u>cis</u> Pd			
Bond	$\Delta$ ( $\overset{\circ}{\text{A}}$ )		
Pd-P	- 0.073		
Pd-Cl	+ 0.075		

---

---

Pt <u>trans</u>			
Bond	Distance ( $\overset{\circ}{\text{A}}$ )	Compound	Ref.
Pt-P	$2.315 \pm 0.004$	Pt $\text{P}(\text{C}_2\text{H}_5)_3 \text{Br}$	28
Pt-Cl	$2.294 \pm 0.009$	Pt $\text{P}(\text{C}_2\text{H}_5)_3 \text{Cl}_2$	28

Pt <u>cis</u>			
Bond	Distance ( $\overset{\circ}{\text{A}}$ )	Compound	Ref.
Pt-P	$2.247 \pm 0.008$	$\text{PtCl}_2(\text{P}(\text{CH}_2)_3)_2$	29
Pt-Cl	$2.376 \pm 0.009$	"	

^ <u>trans</u> to <u>cis</u> Pt	
Bond	$\Delta$ ( $\overset{\circ}{\text{A}}$ )
Pt-P	- 0.068
Pt-Cl	+ 0.082

---



the M-Cl and M-P distances are somewhat different. However, the changes in the bond distances are identical within 1 e.s.d. in going from the trans to the cis configuration.

STRUCTURE OF  
NITRILOTRIACETODIAQUOPRASEODYMIUM(III)-MONOHYDRATE

Introduction

The complexes formed by the reaction of the trivalent lanthanons with nitrilotriacetate (NTA) in aqueous solution have been studied for some time.<sup>30</sup> The crystalline complexes formed by precipitation from saturated solution have been found to form one of several hydrates depending upon the temperature at which recrystallization is carried out and the rare earth used. Our preliminary study of the series of complexes formed at 25° C indicates that the series is divided into three crystallographically distinct groups: (1) the La-Ce group, (2) the Pr-Tb (Pm?) group and (3) the Dy-Lu group. Crystals of the first group are so poorly formed that they could not be characterized. Crystals of the second group belong to the space group Pbc<sub>a</sub> with  $\underline{a} = 13.21 \pm 0.01$ ,  $\underline{b} = 29.98 \pm 0.01$  and  $\underline{c} = 8.132 \pm 0.006 \text{ \AA}$ . Those of the third group are in space group Pca2<sub>1</sub> with  $\underline{a} = 21.535 \pm 0.013 \text{ \AA}$ ,  $\underline{b} = 9.02 \pm 0.004 \text{ \AA}$ ,  $\underline{c} = 12.186 \pm 0.007 \text{ \AA}$ .

This division into groups also coincides with observed changes in hydration number across the series from 5 to 3 to 4.<sup>31</sup> The break between groups at Tb occurs near a sudden change in thermodynamic properties of these as well as other lanthanon (III) complexes.<sup>32</sup> Coordination numbers ranging from 6 to 12 have been observed in various com-

plexes.<sup>33-36</sup> The smaller coordination numbers are usually associated with the heavier rare earths while coordination numbers of 9 or greater are not uncommon for the light rare earths. We therefore undertook a three-dimensional X-ray structural study of  $\text{Pr}(\text{NTA}) \cdot 3\text{H}_2\text{O}$  in order to determine its coordination. In the next chapter the structure of  $\text{Dy}(\text{NTA}) \cdot 4\text{H}_2\text{O}$  is described.

### Experimental

Well formed, rectangular prismatic crystals of the  $\text{Pr} \cdot \text{NTA} \cdot 3\text{H}_2\text{O}$  complex (M.W. = 383.1 g), were kindly supplied by J. E. Powell of this Laboratory. Preliminary Weissenberg and precession photographs indicated orthorhombic symmetry. Systematic absences were observed for  $0k1$ ,  $k$  odd;  $h01$ ,  $l$  odd;  $hk0$ ,  $h$  odd and are consistent with space group  $\text{Pbca}$  ( $D_{2h}^{15}$ ). Accurate unit cell parameters were obtained from a least-squares fit of 16 independent reflections whose  $2\theta$  values were obtained from Weissenberg photographs calibrated with Al powder using  $\text{CuK}\alpha$  radiation ( $\lambda = 1.54051 \text{ \AA}$ ). The unit cell parameters and their standard deviations calculated from the inverse matrix are  $a = 13.21 \pm 0.01$ ,  $b = 20.98 \pm 0.01$ ,  $c = 8.132 \pm 0.006 \text{ \AA}$  and  $v = 2254 \text{ \AA}^3$ . The density determined by flotation techniques in a diiodomethane-1-bromopropane mixture is 2.24 g/cc, while the calculated density with  $Z = 8$  is 2.26 g/cc.

A crystal having approximate dimensions 0.07 x 0.05 x

0.26 mm was mounted so that its long axis (100) was coincident with the phi axis of the diffractometer. A General Electric, XRD-6, X-ray diffractometer equipped with single crystal orienter and scintillation counter was used with Zr-filtered, MoK $\alpha$  radiation ( $\lambda = 0.717 \text{ \AA}$ ) in the moving-crystal-moving-counter mode ( $\theta.2\theta$  coupled) to measure the intensities. A 40 sec scan covering  $1.36^\circ$  in  $2\theta$  was employed with a take-off angle of  $2^\circ$ . Since the background was seen to be a function of  $\theta$  only, individual reflections were obtained from a plot of  $2\theta$  vs. background. One crystallographic independent octant of data was collected within a  $2\theta$  sphere of  $45^\circ$  ( $\sin\theta/\lambda = 0.538$ ). No appreciable decrease in the intensities of three independent reflections which were remeasured periodically throughout the data taking period was observed.

The measured intensities were also corrected for Lorentz and polarization effects and for absorption<sup>7</sup> with minimum and maximum transmission factors of 0.74 and 0.76 ( $\mu = 43.2 \text{ cm}^{-1}$ ). The standard deviations were assigned to the intensities according to the formula:

$$\sigma(I) = (C_t + C_b + (0.05 \times C_t)^2 + (0.10 \times C_b)^2 + (0.05 \times C_n)^2)^{1/2} \times A$$

where  $C_t$ ,  $C_b$ ,  $C_n$  and  $A$  are the total count, background count, net count and absorption factor, respectively. The quadratic

terms correspond to estimated systematic errors of 5, 10, and 5% in the total count, background count, and net count, respectively. The standard deviations of the structure amplitudes ( $\sigma(\underline{F})$ ) were obtained by the method of finite differences.<sup>5</sup> Of the 1494 measured reflections, 368 had a value of  $\underline{F}_0 < 2 \sigma(\underline{F})$ . They were considered to be unobserved and were not included in the refinement.

### Solution of the Structure

The structure was solved by normal heavy atom techniques. The heavy atom was readily located in the Patterson map and the light atoms were found in a series of structure factor-electron density map calculations. Scattering factors used were those of Cromer and Waber<sup>37</sup> for the praseodymium(III) atom corrected for anomalous scattering<sup>22</sup> and those of Hanson et al.<sup>8</sup> for the light atoms. All atoms were refined<sup>6</sup> isotropically to a value of the discrepancy indicator ( $R = \Sigma \Delta / \Sigma |\underline{F}_0|$  where  $\Delta = ||\underline{F}_0| - |\underline{F}_c||$ ) of 0.13. At this point weights were introduced based on the individual statistics of the reflections ( $\underline{w} = 1/\sigma^2(\underline{F})$ ). These weights were later adjusted slightly to remove a dependence of  $\underline{w} \Delta^2$  on  $|\underline{F}_0|$ . In addition, 15 reflections with values of  $\Delta > 6.0 \times \sigma(\underline{F})$  were excluded from the refinement. The large isotropic temperature factor of  $O_{W3}$  suggested occupational disorder. However, refinement of the occupational parameter yielded a value near unity. An attempt was then made to refine all

atoms anisotropically but was aborted when no physically meaningful results were obtained. With only the  $\text{Pr}^{3+}$  anisotropic final values of  $\underline{R}$  and the weighted discrepancy index,  $\underline{R}_w$  ( $\underline{R}_w = \frac{\sum w \Delta^2}{\sum w F_o^2}$ )<sup>1/2</sup>, of 0.085 and 0.080 were obtained. The final difference electron density map contained no residual density greater than  $0.8 \text{ e}^{-/\text{A}^2}$  and confirmed that all nonhydrogen atoms had been located. In Table 7 are listed the final atomic positional parameters and temperature factor coefficients along with their estimated standard deviation (esd) as derived from the inverse matrix.<sup>23</sup> For praseodymium, the maximum, intermediate and minimum root-mean-square amplitudes of vibration are 0.145, 0.144 and 0.135. The magnitudes of the observed and calculated structure factors are shown in Figure 9.

#### Results and Discussion

The configuration of the NTA ligand around the  $\text{Pr}^{3+}$  is shown in Figure 10.<sup>11</sup> There are six carboxylic oxygens ( $\text{O}_c$ ), two waters ( $\text{O}_w$ ) and one nitrogen coordinated to the metal atom. Relevant distances and angles are given in Table 8. There are no discrete molecular units in the complex. One bridge is formed by  $\text{O}_{21}$  by which two different adjacent metal atoms are coordinated. In addition,  $\text{O}_{22}$  and  $\text{O}_{31}$  coordinate to metal atoms other than the one to which the remainder of the NTA ligand is coordinated. Two oxygen atoms  $\text{O}_{w3}$  and  $\text{O}_{12}$  are not coordinated to any metal atom.

Table 7. Fractional atomic coordinates and thermal parameters<sup>a,b</sup>

Atom	X	Y	Z	B <sub>iso</sub> (Å <sup>2</sup> )
N	0.330(1)	0.1444(8)	0.021(2)	2.0(3)
O <sub>11</sub>	0.137(1)	0.1719(8)	0.117(2)	2.4(3)
O <sub>12</sub>	0.158(1)	0.2753(8)	0.073(2)	3.3(3)
C <sub>11</sub>	0.307(2)	0.211(1)	0.073(3)	2.3(4)
C <sub>12</sub>	0.190(2)	0.220(1)	0.089(3)	2.5(4)
O <sub>21</sub>	0.283(1)	0.0271(6)	-0.105(2)	1.8(3)
O <sub>22</sub>	0.328(1)	0.0551(7)	-0.352(2)	3.1(3)
C <sub>21</sub>	0.307(2)	0.137(1)	-0.154(3)	2.7(4)
C <sub>22</sub>	0.307(1)	0.0691(9)	-0.204(2)	1.4(3)
O <sub>31</sub>	0.541(1)	0.0544(7)	0.201(2)	2.6(3)
O <sub>32</sub>	0.377(1)	0.0410(6)	0.219(2)	2.2(3)
C <sub>32</sub>	0.452(2)	0.072(1)	0.171(3)	2.8(4)
C <sub>31</sub>	0.441(2)	0.130(1)	0.055(3)	2.6(5)
O <sub>w1</sub>	0.252(1)	0.1286(7)	0.409(2)	2.7(3)

<sup>a</sup>Estimated standard deviations are given in parentheses right adjusted to the least significant figure of the preceding number.

<sup>b</sup>Anisotropic temperature factors are given for Pr only. They are times 10<sup>3</sup> and have the form

$$\exp[-(\underline{a}_{11} \underline{h}^2 + \underline{a}_{22} \underline{k}^2 + \underline{a}_{33} \underline{l}^2 + \underline{a}_{12} \underline{hk} + \underline{a}_{13} \underline{hl} + \underline{a}_{23} \underline{kl})].$$

Table 7. (Continued)

Atom	X	Y	Z	$B_{iso} (\text{\AA}^2)$	
O <sub>W2</sub>	0.076(1)	0.0576(8)	-0.075(2)	3.0(3)	
O <sub>W3</sub>	0.508(2)	0.299(1)	0.183(3)	7.2(5)	
Pr	0.19901(8)	0.06427(5)	0.16546(13)		
$B_{11}$	$B_{22}$	$B_{33}$	$B_{12}$	$B_{13}$	$B_{23}$
234(7)	83(3)	619(19)	6(4)	-1(13)	-8(8)



Figure 9. Observed and calculated structure factors (in electrons times 10)  
for  $\text{Pr}\cdot\text{N}(\text{C}_2\text{H}_2\text{O}_2)_3\cdot 3\text{H}_2\text{O}$



Figure 10. The perspective drawing of nitrilotriacetate-triaquopraseodymium III-mono hydrate. (The numbering in the NTA ligand is such that the left number indicates the acetate group to which the atom belongs. In the case of the carbon atoms the right number indicates its position relative to the nitrogen and in the case of the oxygen atoms, is solely for uniqueness. The primes indicate atoms related to those of the coordinate list by symmetry operations which are described elsewhere)

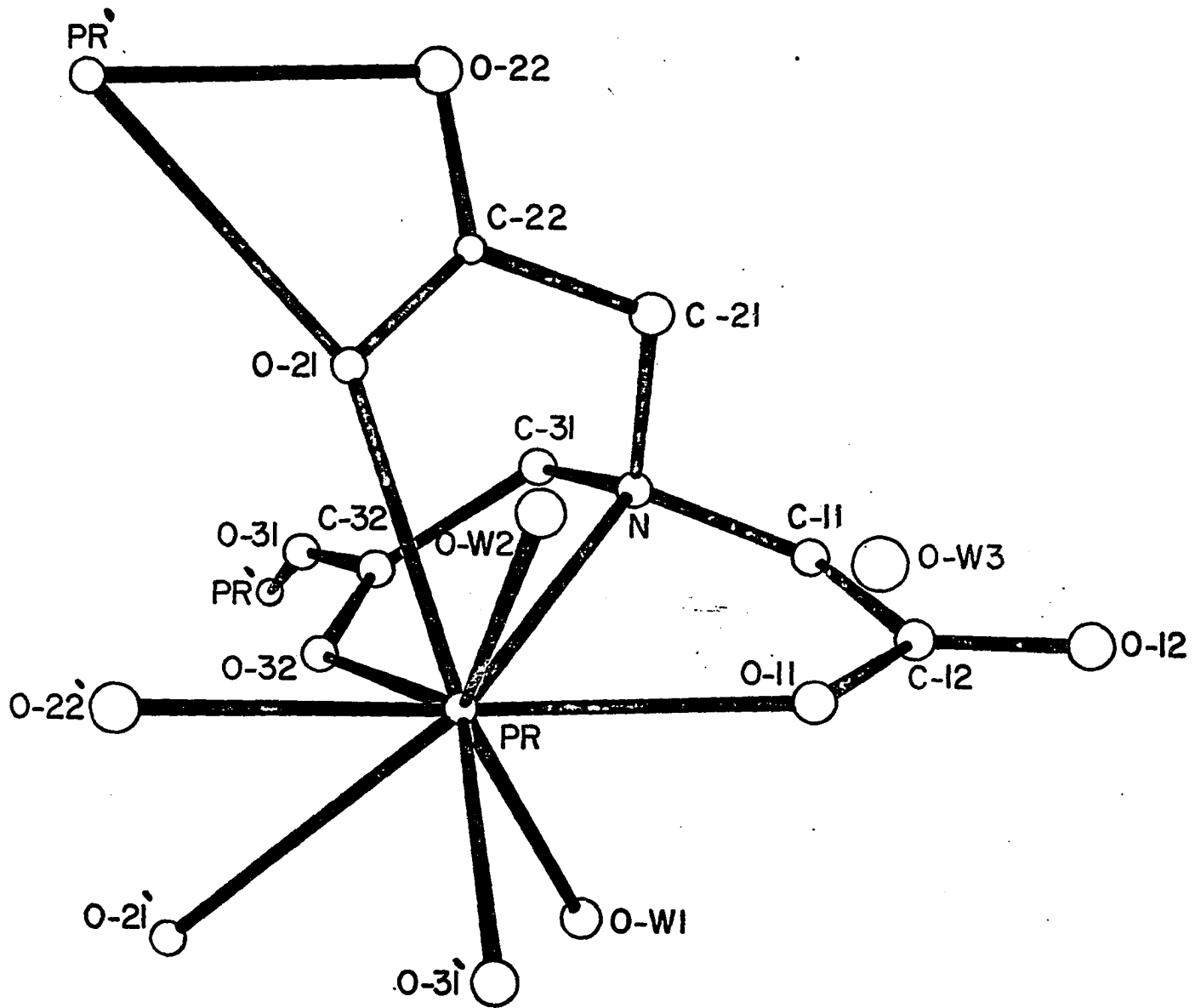


Table 8. Selected distances ( $\text{\AA}$ ) and angles (deg) with associated standard errors as calculated from the parameters in Table 7<sup>a</sup>

Distances					
Pr-O <sub>11</sub>	2.43(1)	N-C <sub>11</sub>	1.48(2)	C <sub>22</sub> -O <sub>22</sub>	1.27(2)
Pr-O <sub>21</sub>	2.59(1)	N-C <sub>21</sub>	1.49(3)	C <sub>32</sub> -O <sub>31</sub>	1.25(2)
Pr-O <sub>21</sub> <sup>1</sup>	2.69(1)	N-C <sub>31</sub>	1.53(3)	C <sub>32</sub> -O <sub>32</sub>	1.25(2)
Pr-O <sub>22</sub> <sup>1</sup>	2.53(1)	C <sub>11</sub> -C <sub>22</sub>	1.57(3)	O <sub>12</sub> -O <sub>w3</sub> <sup>2</sup>	2.85(3)
Pr-O <sub>31</sub> <sup>2</sup>	2.37(1)	C <sub>21</sub> -C <sub>22</sub>	1.47(3)	O <sub>12</sub> <sup>3</sup> -O <sub>w3</sub> <sup>2</sup>	2.72(2)
Pr-O <sub>32</sub>	2.44(1)	C <sub>31</sub> -C <sub>32</sub>	1.55(3)	O <sub>21</sub> -O <sub>w2</sub>	2.82(2)
Pr-O <sub>w1</sub>	2.50(1)	C <sub>12</sub> -O <sub>11</sub>	1.25(2)	O <sub>32</sub> -O <sub>w2</sub> <sup>1</sup>	2.73(2)
Pr-O <sub>w2</sub>	2.54(1)	C <sub>12</sub> -O <sub>22</sub>	1.24(2)	O <sub>21</sub> -O <sub>22</sub>	2.18(2)
Pr-N	2.68(2)	C <sub>22</sub> -O <sub>21</sub>	1.24(2)	O <sub>11</sub> -O <sub>12</sub>	2.21(2)
				O <sub>31</sub> -O <sub>32</sub>	2.19(2)

<sup>a</sup>Superscripts indicate symmetry operations which relate the atom to the original coordinates: 1)  $1/2 - x, \bar{y}, 1/2 + z$ ; 2)  $-1/2 + x, y, 1/2 - z$ ; 3)  $x, 1/2 - y, 1/2 + z$ ; 4)  $1/2 - x, \bar{y}, -1/2 + z$ ; 5)  $1/2 + x, y, 1/2 - z$ .

Table 8. (Continued)

		Angles around Pr			
$O_{11}^2-Pr-O_{31}^2$	82.0(5)	$O_{31}^2-Pr-O_{21}$	138.1(4)	$O_{w2}-Pr-O_{22}^1$	79.1(5)
$O_{11}-Pr-O_{w1}$	73.9(4)	$O_{31}^2-Pr-O_{22}^1$	79.3(5)	$O_{w2}-Pr-O_{21}^1$	123.4(4)
$O_{11}-Pr-O_{w2}$	73.3(5)	$O_{31}^2-Pr-O_{21}^1$	72.3(4)	N-Pr-O <sub>32</sub>	65.3(5)
$O_{11}-Pr-N$	64.1(5)	$O_{w1}-Pr-O_{w2}$	145.0(5)	N-Pr-O <sub>21</sub>	62.6(5)
$O_{11}-Pr-O_{32}$	122.5(5)	$O_{w1}-Pr-N$	80.0(5)	N-Pr-O <sub>22}^1</sub>	133.3(5)
$O_{11}-Pr-O_{21}$	106.6(4)	$O_{w1}-Pr-O_{32}$	72.2(4)	N-Pr-O <sub>21}^1</sub>	134.0(4)
$O_{11}-Pr-O_{22}^1$	149.4(5)	$O_{w1}-Pr-O_{21}$	135.8(4)	$O_{32}-Pr-O_{21}$	71.3(4)
$O_{11}-Pr-O_{21}^1$	143.6(4)	$O_{w1}-Pr-O_{22}^1$	128.2(5)	$O_{32}-Pr-O_{22}^1$	87.1(4)
$O_{31}^2-Pr-O_{w1}$	86.1(5)	$O_{w1}-Pr-O_{21}^1$	79.0(4)	$O_{32}-Pr-O_{21}^1$	69.4(4)
$O_{31}^2-Pr-O_{w2}$	77.6(5)	$O_{w2}-Pr-N$	96.3(5)	$O_{21}-Pr-O_{21}^1$	109.8(1)
$O_{31}^2-Pr-N$	145.7(5)	$O_{w2}-Pr-N$	137.8(5)	$O_{21}-Pr-O_{22}^1$	73.4(4)
$O_{31}^2-Pr-O_{32}$	138.7(4)	$O_{w2}-Pr-O_{21}$	66.7(4)	$O_{21}-Pr-O_{22}$	49.2(4)

Table 8. (Continued)

Angles in NTA ligand					
$C_{11}-N-C_{21}$	110(2)	$N-C_{31}-C_{32}$	111(2)	$C_{21}-C_{22}-O_{22}$	119(2)
$C_{11}-N-C_{31}$	109(2)	$C_{11}-C_{12}-O_{11}$	118(2)	$O_{21}-C_{22}-O_{22}$	120(2)
$C_{21}-N-C_{31}$	110(2)	$C_{11}-C_{12}-O_{22}$	117(2)	$C_{31}-C_{32}-O_{31}$	116(2)
$N-C_{11}-C_{12}$	110(2)	$O_{11}-C_{12}-O_{22}$	126(2)	$C_{31}-C_{32}-O_{32}$	122(2)
$N-C_{21}-C_{22}$	112(2)	$O_{21}-C_{22}-O_{21}$	120(2)	$O_{31}-C_{32}-O_{32}$	122(2)
Angles involving NTA and Pr					
$C_{12}-O_{11}-Pr$	126(1)	$C_{22}-O_{22}-Pr^4$	98(1)	$C_4-N-Pr$	110(1)
$C_{22}-O_{21}-Pr$	117(1)	$C_{31}-O_{31}-Pr^2$	153(1)	$C_{21}-N-Pr$	103(1)
$C_{22}-O_{21}-Pr^4$	92(1)	$C_{31}-O_{32}-Pr$	128(1)	$C_{31}-N-Pr$	115(1)

Thus two of the six  $O_c$ 's in each NTA molecule are coordinated to the same metal atom as the nitrogen, two are coordinated to adjacent metal atoms, one is simultaneously coordinated to two adjacent metal atoms and the last is uncoordinated.

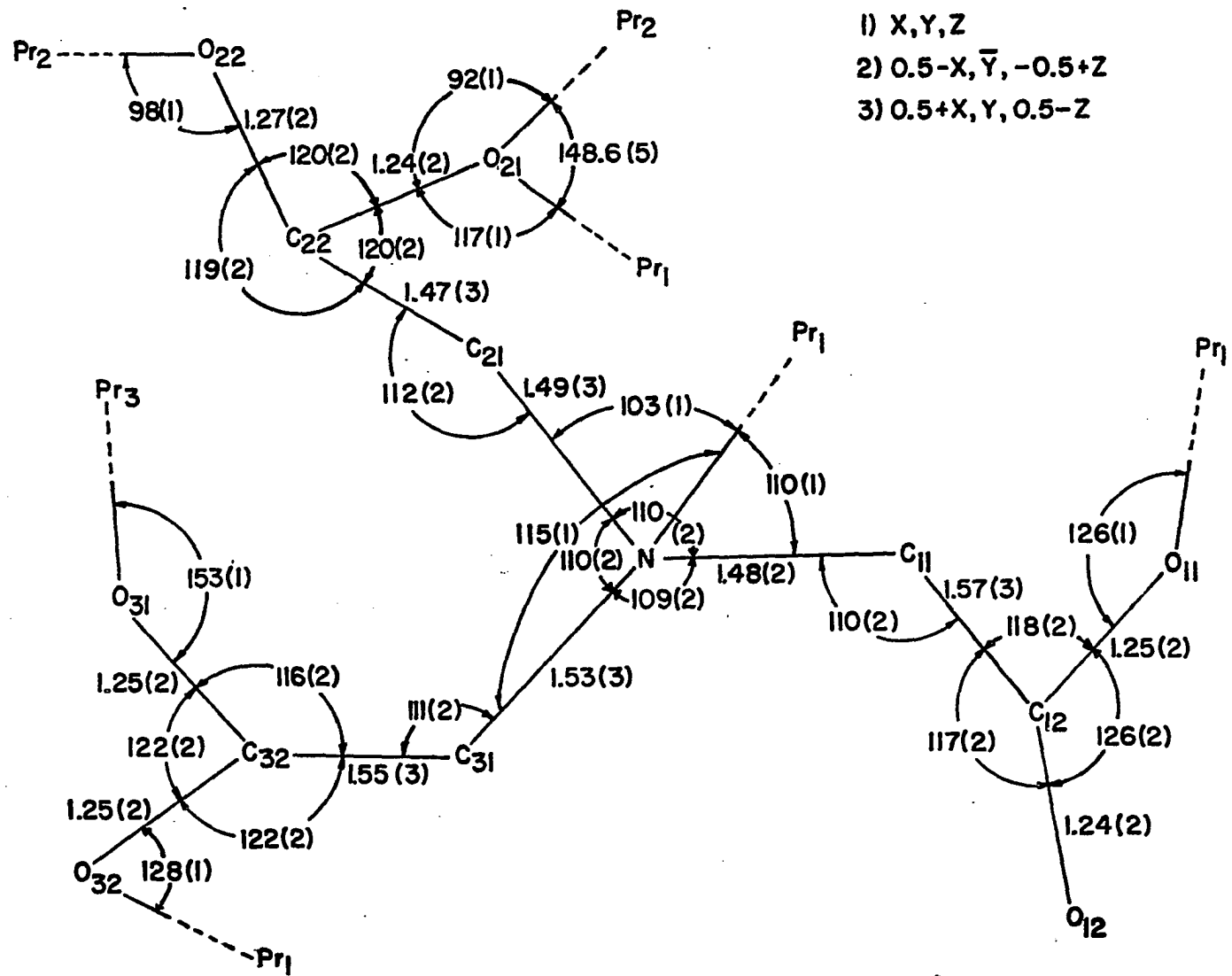
The average for the six independent terminal carbon to carboxylic oxygen bond distances is  $1.25 \pm 0.02 \text{ \AA}$ . This is in excellent agreement with the expected value for the C-O distance in a carboxylate ion.<sup>38,39</sup> Moreover, none of the C-O distances vary from this value by more than one esd which indicates the acid is completely deprotonated and that the  $O_{12}-C_{12}$  bond ( $1.24 \pm 0.02 \text{ \AA}$ ) has no significantly greater double bond character than the rest. The three acetate groups are planar to within  $0.1 \text{ \AA}$ , while the angles around the carboxylate carbons are  $120^\circ \pm 3^\circ$  with the exception of the  $O_{11}-C_{12}-O_{12}$  angle which is slightly larger ( $126 \pm 2^\circ$ ). This increase in angle can be attributed to steric strain in the unsymmetric environment caused by single coordination of this carboxylate group. The angles around the nitrogen are essentially tetrahedral with the "lone pair" directed approximately towards the metal atom (see Figure 11).

There are four short  $O_w-O_c$  distances ranging from 2.72 to  $2.85 \text{ \AA}$  which are suggestive of possible hydrogen bond formation. The large thermal parameters of  $O_w3$  suggests that it is involved in only a weak hydrogen bond.

The arrangement of the atoms in the coordination sphere



Figure 11. The conformation of the NTA ligand (bond distances ( $\text{\AA}$ ) and angles (deg) are shown along with their estimated errors right adjusted to the least significant figure of the preceding number. The subscripts of the Pr atoms indicate their relation to the Pr in the coordinate list)

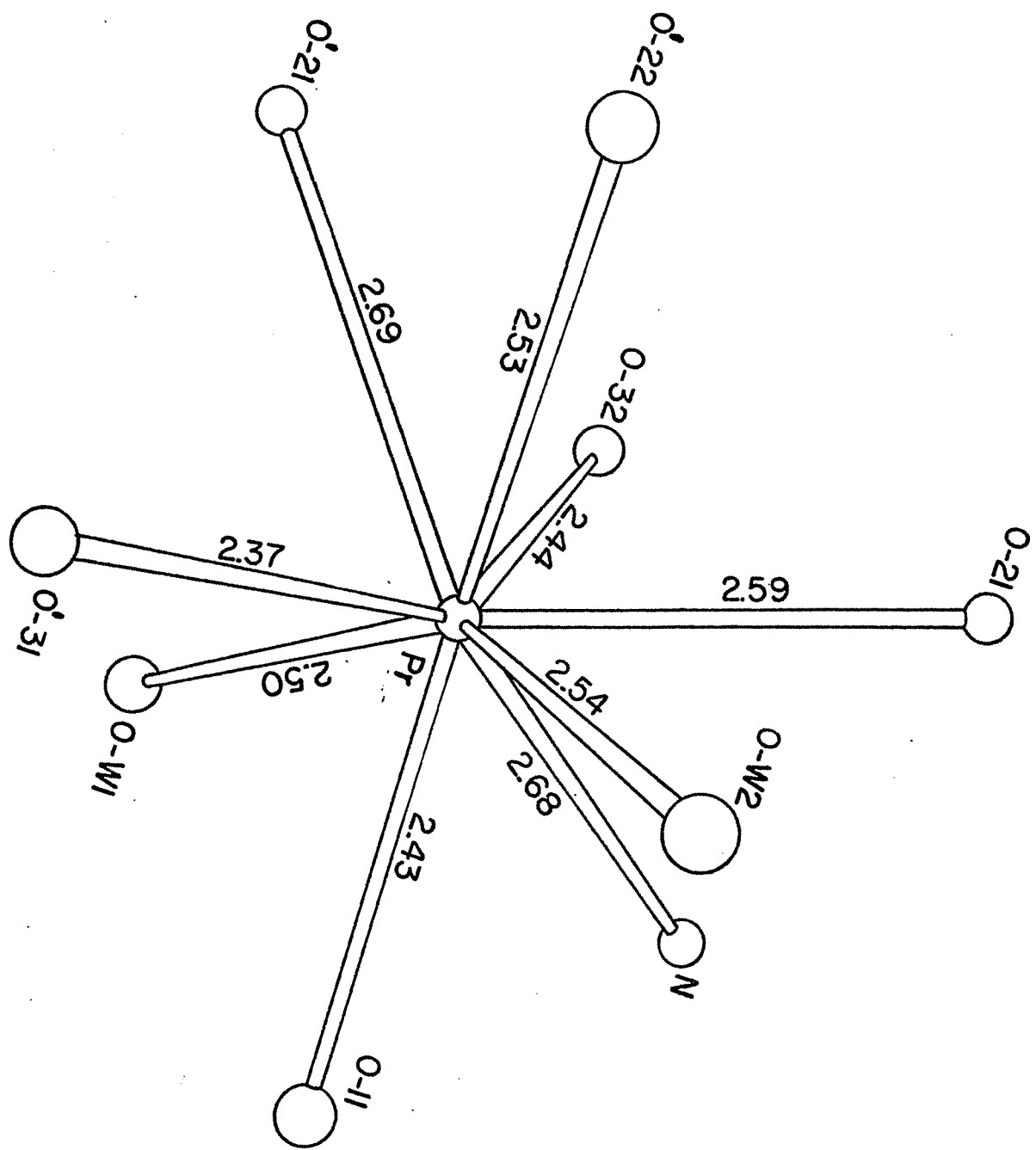


is shown in Figure 12. The average Pr-O<sub>c</sub> distance is  $2.47 \pm 0.02 \text{ \AA}$  while the average Pr-O<sub>w</sub> distance is  $2.52 \pm 0.02 \text{ \AA}$ .

The Pr-O<sub>21</sub> distances have been excluded from this calculation since they are significantly longer than the other Pr-O<sub>c</sub> distances due to the different coordination mode exhibited by O<sub>21</sub>. The Pr-N distance is  $2.68 \pm 0.02 \text{ \AA}$ . The average metal-oxygen distance is in reasonable agreement with the value predicted either from the sum of the covalent radii<sup>24</sup> or from the sum of the crystal radii.<sup>40</sup> The Pr-N distance is  $\sim 0.1 \text{ \AA}$  longer than would be expected, indicating weaker coordination. These values are  $0.04$  to  $0.08 \text{ \AA}$  shorter than those observed by Hoard et al.<sup>41</sup> in the nine coordinate La.EDTA complex ( $2.51 \text{ \AA}$ ,  $2.58 \text{ \AA}$ ,  $2.76 \text{ \AA}$  for the average La-O<sub>c</sub>, La-O<sub>w</sub> and La-N distances). This general shortening is consistent with a decrease in the rare earth ionic radius from  $1.15 \text{ \AA}$  to  $1.09 \text{ \AA}$ . In fact, assuming the average oxygen-metal-oxygen angle remains constant ( $72$  to  $74^\circ$ ), a continued decrease in the metal-oxygen bond distance of  $0.10 \text{ \AA}$  to  $0.14 \text{ \AA}$  would cause significant oxygen-oxygen steric interactions. This would occur at Dy<sup>3+</sup> ( $0.99 \text{ \AA}$ ) or Ho<sup>3+</sup> ( $0.97 \text{ \AA}$ ) and a change in coordination number from 9 to 8 would be expected.

The arrangement of atoms around the Pr<sup>3+</sup> can be described equally well in any of three ways: (1) as a distorted, tri-capped trigonal prism, (2) as a capped square anti-prism or (3) as in the description by Hoard et al. of

Figure 12. A perspective drawing of the Pr coordination. (The orientation is the same as in Figure 11. The primes indicate atoms related to those in the coordinates list: (1)  $O_{21}'$ :  $1/2 - x, \bar{y}, 1/2 + z$ , (2)  $O_{22}'$ :  $1/2 - x, \bar{y}, 1/2 + z$  and (3)  $O_{31}'$ :  $-1/2 + x, y, 1/2 - z$ )



the La·EDTA complex.

The tri-capped, trigonal prism arrangement has been observed for many nona-coordinate structures and have been described in some detail in a review by Muetterties and Wright.<sup>42</sup> Typical of these are the anhydrous, rare earth tri-chlorides.<sup>43</sup> Referring to Figure 12, the three rectangular faces of the trigonal prism are as follows:  $O_{22}'-O_{32}'-N-O_{w2}-O_{22}'$ ,  $O_{w2}-N-O_{w1}-O_{31}'-O_{w2}$ , and  $O_{31}'-O_{w1}-O_{32}'-O_{22}'-O_{31}'$ . The two triangular faces of the prism are described by  $O_{22}'-O_{w2}-O_{31}'-O_{22}'$  and  $O_{32}'-N-O_{w1}-O_{32}'$ . The atoms  $O_{21}$ ,  $O_{21}'$  and  $O_{11}$  occupy the capping positions.

The capped square anti-prism is observed somewhat less frequently than is the tri-capped trigonal prism;<sup>42</sup> however, the square anti-prism is a very common arrangement for octa-coordination. In Figure 12, the rectangular faces of the square anti-prism are defined by  $O_{22}'$ ,  $O_{32}'$ ,  $O_{w1}$ ,  $O_{31}'$ ,  $O_{22}'$  and  $O_{21}$ ,  $N$ ,  $O_{11}$ ,  $O_{w2}$ ,  $O_{21}$ . The atom in the capping position ( $O_{21}'$ ) shows a significant distortion towards  $O_{22}'$ .

The description favored by Hoard et al.<sup>41</sup> for the nona-coordinate La·EDTA complex, due to the large distortions from any regular geometric figure, is a one, five, three arrangement where one atom ( $O_{31}'$ ) is located  $1.9 \pm 0.2 \text{ \AA}$  below a plane of five atoms,  $O_{21}'$ ,  $O_{22}'$ ,  $O_{w2}$ ,  $O_{11}$ ,  $O_{w1}$ . The equation of this plane along with selected distances from the plane are given in Table 9. The average O-Pr-O angle in

Table 9. Selected distances to and equations of the planes

Atom	Distance $\overset{\circ}{\text{O}}$ from plane (Å)	Atom	Distance $\overset{\circ}{\text{O}}$ from plane (Å)
Plane 1			
O <sub>22</sub>	0.22	O <sub>31</sub>	1.90
O <sub>21</sub>	0.23	Pr	0.46
O <sub>w1</sub>	0.14	N	2.54
O <sub>11</sub>	0.06	O <sub>21</sub>	2.47
O <sub>w2</sub>	0.05	O <sub>32</sub>	2.31
Equation:			
$(0.881)x + (0.005)y - (0.474)z - 1.229 = 0$			
Plane 2			
O <sub>21</sub>	0.0	O <sub>22</sub>	2.10
O <sub>32</sub>	0.0	O <sub>21</sub>	2.44
N	0.0	O <sub>w1</sub>	2.23
O <sub>31</sub>	4.31	O <sub>11</sub>	2.66
Pr	1.97	O <sub>w2</sub>	2.61
Equation:			
$(0.907)x - (0.052)y - (0.418)z - 3.720 = 0$			

the plane is  $71^\circ$  while the average O-O distance is  $2.97 \text{ \AA}$ . The most significant distortions from these averages occur in the  $O_{22}'\text{-Pr-O}_{21}'$  angle of  $49.2^\circ$  and  $O_{21}'\text{-O}_{22}'$  distance of  $2.18 \pm 0.02 \text{ \AA}$ . This appears to be a result of both carboxylate oxygens being in the same acid moiety. The  $\text{Pr}^{3+}$  is located  $0.5 \text{ \AA}$  above the approximate center of this plane away from the  $O_{31}'$ . In the  $\text{La}\cdot\text{EDTA}$  complex, the distance from the similar plane to  $\text{La}^{3+}$  is  $0.6 \text{ \AA}$ ; some increase being expected due to the longer oxygen- $\text{La}^{3+}$  distances.

At a distance of  $2.0 \text{ \AA}$  from the  $\text{Pr}^{3+}$  and opposite the first plane is a second plane of three atoms:  $O_{21}$ , N,  $O_{32}$ . The equation of this plane and some selected distances from the plane are given in Table 9. The two planes are within  $9^\circ$  of being parallel.

In complexes such as ceric ammonium nitrate<sup>44</sup> considerable distortion of the N-O bonds and O-N-O angles have been observed and have been attributed to the presence of metal-oxygen covalent bonding. However, in the  $\text{La}\cdot\text{EDTA}^-$  complex the bonding has been described as primarily electrostatic in nature. In the title compound no systematic distortions in C-O distances or O-C-O angles are observed. This, coupled with the wide range in Pr-O-C angles ( $92^\circ$  to  $153^\circ$ ), would imply primarily electrostatic bonding effects.



STRUCTURE OF  
NITRILOTRIACETODIAQUODYSPROSIUM(III)-DIHYDRATE

Introduction

The diversity in types of coordination found in the rare-earth complexes is large (45-49). In an endeavor to determine the effect of changing metal-ion size on coordination, we have investigated the structures of the lanthanon (III)-nitrilotriacetate (NTA) complexes from Pr-Lu. The series is broken into two groups--the Pr group and the Dy group. In the previous chapter the structure of the Pr group has been discussed. In this chapter the structure of the Dy NTA complex will be discussed and comparisons made to the Pr structure.

Experimental

Well formed rectangular-prismatic crystals of  $\text{Dy} \cdot \text{NTA} \cdot 4\text{H}_2\text{O}$  (M.W. = 422.7 g) were supplied by J. E. Powell and were used without additional purification. Weissenberg and precession photographs indicated an orthorombic space group with systematic extinctions of the type  $0k1$ ,  $l$  odd and  $h0l$ ,  $h$  odd. These conditions indicate the space group to be either  $\text{Pca}2_1$  or  $\text{Pcam}$  (No. 57-Pbcm). In addition the  $0k0$ ,  $k$  odd reflections were unobserved. However, there are no special positions in  $\text{Pca}2_1$  or  $\text{Pcam}$  which can account for this type of extinction. The light lanthanon(III) NTA com-

plexes crystallize in space  $Pbca$ , and  $Pca2_1$  can be obtained from  $Pbca$  by removal of the center of symmetry, interchanging the  $a$  and  $b$  axes, and translation of the origin to the  $2_1$ . In addition, the  $0k0$  extinction condition suggests that the  $y, 1/2 + y$  relationship has been retained from  $Pbca$ . Therefore, it was decided to initially assume  $Pca2_1$  as the space group, which was later justified by successful refinement in this space group.

The unit cell dimensions were determined by least-squares fit of 29 independent reflections whose  $2\theta$  values were obtained from Weissenberg photographs calibrated with Al powder lines at  $25^\circ C$  using Cu-K $\alpha$  radiation ( $\lambda = 1.5405 \text{ \AA}$ ). The values obtained along with the estimated errors are:  $a = 21.535 \pm 0.013 \text{ \AA}$ ,  $b = 9.028 \pm 0.004 \text{ \AA}$ ,  $c = 12.186 \pm 0.007 \text{ \AA}$  and  $V_c = 2369 \text{ \AA}^3$ . The measured density was 2.3 g/cc while the calculated density with eight molecules per unit cell is 2.4 g/cc.

A crystal with approximate dimensions 0.12 x 0.12 x 0.26 mm was selected for use in data collection. The crystal was mounted along its long axis with the (001) axis coincident with the phi axis of the diffractometer. Data were collected at room temperature using a Hilger-Watts, four circle diffractometer equipped with a scintillation counter employing Zr-filtered Mo-K $\alpha$  ( $\lambda = 0.7107 \text{ \AA}$ ) radiation. All data in one octant within a  $2\theta$  sphere of  $60^\circ$  ( $\sin\theta/\lambda =$

0.70) were measured using a  $\theta$ - $2\theta$  coupled scan with a  $5^\circ$  take-off angle. Stationary counter measurements of the background were made at the beginning and the end of each scan. The scan range was over 50 steps of  $0.01^\circ$ , one step per 0.4096 sec., increased by 1 step per deg in  $2\theta$  to insure complete integration over the entire peak. The length of the background measurements were adjusted accordingly. No appreciable decrease in the intensities of three standard reflections which were remeasured periodically throughout the data taking period was observed.

The measured intensities were corrected for Lorentz and polarization effects and for absorption<sup>8</sup> with minimum and maximum transmission factors of 0.43 and 0.47 ( $\mu = 65.5 \text{ cm}^{-1}$ ). The standard deviations were assigned to the intensities according to the following formula:

$$\sigma(I) = (C_t + C_b + (0.03 \times C_t)^2 + (0.06 \times C_b)^2 + (0.06 \times C_n)^2)^{1/2} \times A$$

where  $C_t$ ,  $C_b$ ,  $C_n$  and  $A$  represent the total count, background count, net count and the absorption factor, respectively.

The quadratic terms correspond to the estimated systematic errors in the intensity, background, and absorption correction of 3, 6, and 6% respectively. The standard deviations in the structural amplitudes were obtained by the method of finite differences,<sup>5</sup>  $\sigma(\underline{F}) = ((I + (\underline{I}))^{1/2} - \underline{I}^{1/2})/(\underline{L}_p)^{1/2}$ , where

$L_p$  is the Lorentz-polarization factor. Of the 3407 measured reflections, 375 had values of  $F$  less than  $\sigma(F)$  and were considered to be unobserved. They were not used in the refinement.

### Solution of the Structure

The structure was determined using a combination of heavy atom and superposition<sup>50</sup> techniques. Since the space group  $Pca2_1$  has only four general positions, two independent molecules must be present in the unit cell. From the Patterson map the two heavy atom positions were readily located. However, due to the placement of the heavy atoms at almost exactly 0 and 1/2 in  $y$ , the phasing was such that two sets of light atoms appeared in the electron density maps which were related by mirroring at 0 and 1/2 in the  $y$  direction. Because of the large number of light atoms and their small individual contributions to the scattering, it was very difficult to consistently select atoms in the same image. Therefore, a superposition procedure was used starting with a known heavy atom vector. This superposition enabled us to locate single heavy atom-light atom vectors around the heavy atoms. A second superposition eliminated a number of the pseudo peaks. Using vectors from this second superposition, two more superpositions were carried out. The resultant map had, in addition to the peaks corresponding to the heavy atoms, seven peaks which appeared at chemically reasonable

positions for oxygen atoms. By successive electron density map-structure factor calculations, the remaining light atoms positions were determined. In the process, it was found that all but one of the original seven light atoms were correct. Scattering factors used were those of Cromer and Waber<sup>37</sup> for dysprosium<sup>3+</sup> corrected for anomalous scattering<sup>22</sup> and those of Hanson et al.<sup>8</sup> for the light atoms.

All atoms were refined<sup>6</sup> isotropically with unit weights resulting in a value for the discrepancy factor,  $R = \Sigma ||\underline{F}_O| - |\underline{F}_C|| / \Sigma |\underline{F}_O|$  of 0.089. Weights were then introduced based on the individual statistics of the reflections ( $\underline{w} = 1/\sigma^2(\underline{F})$ ). In addition, 65 reflections were removed from the refinement since they did not fulfill the requirement  $||\underline{F}_O| - |\underline{F}_C|| < 9 \times \sigma(\underline{F})$ . The refinement was continued with anisotropic temperature factors for the dysprosium atoms to an  $R$  of 0.057 and of the weighted discrepancy factor  $R_w = (\Sigma \underline{w} (|\underline{F}_O| - |\underline{F}_C|)^2 / \Sigma \underline{w} \underline{F}_O^2)^{1/2}$  of 0.082. In order to further refine the structure, it was necessary to use a variation of a block diagonal procedure. In successive cycles, the parameters of one and then the other of the independent molecules were allowed to vary with all temperature factors anisotropic. This procedure seemed appropriate since the correlation matrix in the isotropic refinement had indicated that the interaction between atoms in nonequivalent molecules were small. In addition, in two final cycles of refinement,

first all positional parameters, and then all temperature factors were allowed to vary to minimize as much as possible any dependence of the parameters on intermolecular correlations. In these two final cycles no parameter shift was greater than 0.5 of the associated estimated standard deviation (esd). Final values of  $\underline{R}$  and  $\underline{R}_w$  were 0.050 and 0.070. A final difference electron density map showed no residual electron density greater than  $0.5 \text{ e}^-/\text{\AA}^3$ .

An attempt was made to determine the absolute configuration of the molecules. One image, the positional parameters of which are listed in Table 10, gave a value of  $\underline{R}$  0.1 lower than the other image, which suggests the former to be the correct configuration. A larger difference was not observed due to the approximate centrosymmetric relationship between the two independent molecules. The independence of the two molecules is indicated by the fact that only 8 out of a possible 108 correlations between terms related by the approximate centering had values greater than 0.1 and no term exceeded 0.36.

Previous experience on the trisilane structure using a  $9 \times 9$  block diagonal procedure indicated that the method may lead to an underestimate of the esd's by 0.20. This is probably a maximum value for the esd's in Table 10 since much larger blocks were used. In Table 11 are listed the root-mean-square amplitudes of vibration while in Figure 13

Table 10. Atom positions and anisotropic temperature factors<sup>a</sup>

Atom	x	y	z	$\beta_{11}$
Dy1	61202(2)	-130(5)	0	60(1)
Dy2	19555(2)	49940(5)	18663(5)	60(1)
O1E1	415(5)	3745(11)	-1868(9)	20(3)
O1E2	166(7)	52(11)	-3300(8)	26(3)
O1D1	889(4)	-2259(9)	748(8)	17(2)
O1D2	1080(4)	-4690(8)	625(8)	14(2)
O1U1	470(4)	456(11)	-203(10)	11(2)
O1U2	-1416(5)	-545(14)	-88(13)	9(2)
C1E1	-43(6)	-205(14)	-2033(11)	17(3)
C1E2	68(6)	-440(15)	-2454(12)	10(3)
C1D1	363(7)	-3673(14)	-628(15)	18(3)
C1D2	810(5)	-3540(12)	363(9)	6(2)
C1U1	-574(6)	-2241(14)	-325(15)	16(3)
C1U2	-847(6)	-636(14)	-181(12)	12(3)
O2E1	2269(5)	5158(8)	3748(8)	15(2)
O2E2	2702(4)	4106(10)	5198(7)	17(2)
O2D1	1450(3)	2723(7)	1796(8)	7(2)
O2D2	1491(5)	496(11)	1067(9)	15(2)
O2U1	3019(3)	5570(10)	1850(10)	7(2)

<sup>a</sup>Heavy atom parameters are times  $10^5$  while light atom parameters are times  $10^4$ .

---

$\beta_{22}$	$\beta_{33}$	$\beta_{12}$	$\beta_{13}$	$\beta_{23}$
380(7)	242(4)	17(2)	-17(2)	-37(4)
421(8)	229(4)	16(2)	-13(2)	-52(4)
85(11)	36(7)	-5(5)	-5(4)	20(8)
169(19)	13(6)	-15(5)	-12(3)	26(8)
68(11)	45(7)	6(4)	-14(33)	-12(7)
28(8)	41(6)	7(3)	-9(3)	-5(6)
79(11)	69(8)	-3(4)	-3(3)	-32(9)
127(15)	135(15)	-1(5)	7(5)	-10(14)
64(15)	50(10)	4(6)	-10(5)	-8(10)
86(15)	39(9)	9(5)	2(4)	-1(11)
74(16)	82(15)	22(6)	-17(6)	-7(13)
55(12)	29(7)	3(4)	-3(4)	-9(8)
52(16)	74(13)	-8(5)	3(5)	-14(12)
59(14)	66(10)	49(5)	6(4)	22(11)
73(11)	26(6)	8(3)	-1(3)	-3(6)
101(13)	29(6)	-1(4)	-4(3)	-23(8)
30(8)	61(7)	1(3)	-1(3)	3(6)
78(10)	57(8)	-10(4)	-17(4)	-10(8)
54(10)	72(8)	12(3)	-9(3)	-5(9)



Table 10. (Continued)

---

Atom	x	y	z	$B_{11}$
O2U2	3997(5)	4988(9)	1811(14)	9(2)
C2E1	2547(6)	2603(13)	3616(11)	13(3)
C2E2	2500(6)	4218(14)	4244(12)	5(2)
C2D1	2402(5)	1415(10)	1905(12)	6(2)
C2D2	1719(5)	1611(13)	1568(9)	9(2)
C2U1	3294(6)	3056(11)	2814(12)	13(3)
C2U2	3444(6)	4659(12)	1941(10)	17(3)
OW11	1501(4)	-633(14)	-1046(10)	8(2)
OW12	634(4)	2596(9)	-232(9)	21(2)
OW21	1100(4)	5684(12)	2951(8)	11(2)
OW22	2041(4)	7570(9)	1705(11)	13(2)
OW13	-2352(5)	1721(12)	-386(14)	14(3)
OW14	-1547(6)	1463(12)	1925(13)	44(4)
OW23	4907(4)	3347(11)	2705(11)	14(2)
OW24	4108(7)	6634(14)	-36(11)	57(6)
N1	41(4)	-2228(9)	-871(8)	14(2)
N2	2625(4)	2764(9)	2460(7)	5(2)

---

---

$\beta_{22}$	$\beta_{33}$	$\beta_{12}$	$\beta_{13}$	$\beta_{23}$
124(15)	97(11)	-13(4)	-9(5)	5(11)
77(15)	45(10)	-5(5)	-10(4)	29(11)
115(17)	38(9)	-7(6)	-7(4)	-2(11)
42(11)	60(10)	-2(4)	-14(4)	-5(10)
64(13)	17(7)	5(5)	-6(3)	-16(8)
28(11)	60(11)	2(4)	5(4)	8(9)
56(12)	12(6)	-1(4)	-4(4)	2(8)
202(18)	66(9)	1(5)	8(3)	-23(12)
41(10)	76(8)	-1(4)	-27(4)	5(8)
161(16)	38(7)	31(5)	-2(3)	-10(9)
46(10)	114(12)	-1(4)	-10(4)	8(10)
169(18)	141(15)	22(6)	-8(5)	58(15)
79(14)	103(12)	12(6)	5(7)	18(12)
96(13)	98(10)	-1(4)	-5(4)	22(10)
136(19)	71(13)	-41(8)	-1(7)	-7(12)
29(10)	29(7)	1(4)	-4(3)	-4(7)
6(10)	21(6)	-9(3)	4(3)	-21(7)

---

Table 11. Root-mean-square thermal displacement ( $\text{\AA}^2$ )

Atom	Min.	Med.	Max.	Atom	Min.	Med.	Max.
Dy1	0.118	0.121	0.144	Dy2	0.115	0.120	0.145
N1	0.115	0.138	0.188	N2	0.078	0.114	0.179
C1E1	0.136	0.179	0.226	C2E1	0.124	0.161	0.230
C1E2	0.130	0.175	0.200	C2E2	0.095	0.181	0.215
O1E1	0.142	0.190	0.241	O2E1	0.141	0.157	0.202
O1E2	0.083	0.229	0.281	O2E2	0.129	0.204	0.220
C1D1	0.091	0.203	0.288	C2D1	0.068	0.136	0.226
C1D2	0.102	0.114	0.179	C2D2	0.091	0.133	0.185
O1D1	0.133	0.174	0.232	O2D1	0.113	0.122	0.212
O1D2	0.104	0.145	0.211	O2D2	0.121	0.173	0.258
C1U1	0.134	0.195	0.240	C2U1	0.105	0.166	0.220
C1U2	0.132	0.165	0.217	C2U2	0.101	0.154	0.195
O1U1	0.133	0.174	0.237	O2U1	0.133	0.153	0.227
O1U2	0.143	0.226	0.325	O2U2	0.130	0.187	0.303
OW11	0.115	0.201	0.309	OW21	0.108	0.170	0.280
OW12	0.130	0.139	0.279	OW21	0.143	0.170	0.296
OW13	0.155	0.252	0.353	OW23	0.177	0.192	0.276
OW14	0.177	0.274	0.319	OW24	0.209	0.236	0.377

Figure 13. Observed and calculated structure factors for  
 $\text{Dy}(\text{N}(\text{C}_2\text{H}_2\text{O}_2)_3)_4\text{H}_2\text{O}$  in electrons x 10





are listed the values of the observed and calculated structure factors. Selected intramolecular distances, both corrected and uncorrected for thermal motion, and angles are given in Table 12. Their estimated errors<sup>23</sup> were determined from the inverse matrix obtained when only the positional parameters were allowed to vary.

### Discussion

The thermal parameters of the atoms in the NTA ligand exhibit a general increase as the distance from the nitrogen increases. Therefore, a correction for thermal motion using a riding model<sup>51</sup> seemed appropriate and was applied to the intraligand distances. Corrections using both a riding model and an independent atom model were made to the metal-oxygen distances.

The molecular configurations of the two independent Dy. NTA·4H<sub>2</sub>O molecules are shown in Figure 14. The two ligands exhibit similar metal coordinations. The three acetate groups in each independent ligand can be placed in one of three categories dependent upon the acetate-oxygen atom (O<sub>a</sub>)-metal atom coordination. For a given ligand, one O<sub>a</sub> atom in each of the three acetate groups, along with the nitrogen atom, coordinate to the same metal atom. Of the remaining three O<sub>a</sub> atoms in each ligand, one is coordinated to an adjacent, symmetry-equivalent dysprosium atom (E type), one is coordinated to an adjacent, nonequivalent metal atom

Table 12. Selected interatomic distances ( $\text{\AA}$ ) and angles (deg)<sup>a</sup>

Atoms	Uncorr.	Riding	Independent
	Metal-light atom distances		
Dy1-O1E1	2.342(10)	2.354	2.368
Dy1-O1E2	2.283(10)	2.304	2.317
Dy1-O1D1	2.303(9)	2.311	2.326
Dy1-O2D2	2.345(9)	2.350	2.373
Dy1-O1U1	2.376(9)	2.385	2.400
Dy1-OW11	2.371(9)	2.392	2.406
Dy1-OW12	2.373(8)	2.386	2.400
Dy1-N1	2.575(9)	2.578	2.592
Dy2-O2E1	2.394(9)	2.401	2.414
Dy2-O2E2	2.307(8)	2.319	2.333
Dy2-O2D1	2.323(7)	2.329	2.343
Dy2-O1D2	2.438(9)	2.453	2.434
Dy2-O2U1	2.348(7)	2.356	2.371
Dy2-OW21	2.352(9)	2.366	2.380
Dy2-OW22	2.341(8)	2.359	2.372
Dy2-N2	2.580(8)	2.580	2.592

<sup>a</sup>Standard deviations are given in parentheses right justified to the last significant figure of the preceding number.



Table 12. (Continued)

Atoms	Uncorr.	Riding	Atoms	Uncorr.	Riding
Intraligand distances					
C1E2-O1E1	1.27(2)	1.28	C2E2-O2E1	1.22(1)	1.22
C1E2-O1E2	1.20(2)	1.23	C2E2-O2E2	1.24(1)	1.25
C1E2-C1E1	1.56(2)	1.56	C2E2-C2E1	1.58(2)	1.58
C1D2-O1D1	1.26(1)	1.27	C2D2-O2D1	1.19(1)	1.20
C1D2-O1D2	1.23(1)	1.24	C2D2-O2D2	1.28(1)	1.30
C1D2-C1D1	1.51(1)	1.53	C2D2-C2D1	1.53(1)	1.53
C1U2-O1U1	1.28(2)	1.29	C2U2-O2U1	1.24(1)	1.25
C1U2-O1U2	1.23(1)	1.27	C2U2-O2U2	1.24(2)	1.27
C1U2-C1U1	1.57(2)	1.57	C2U2-C2U1	1.50(1)	1.50
N1-C1E1	1.44(2)	1.44	N2-C2E1	1.43(2)	1.44
N1-C1D1	1.51(1)	1.53	N2-C2D1	1.47(1)	1.48
N1-C1U1	1.48(2)	1.50	N2-C2U1	1.50(1)	1.51
Intraligand angles					
Atoms		Angles	Atoms		Angles
Intraligand angles					
O2E1-C2E2-O2E2	128(1)		O1E1-C1E2-O1E2	124(1)	
O2E1-C2E2-C2E1	117(1)		O1E1-C1E2-C1E1	119(1)	
O2E2-C2E2-C2E1	115(1)		O1E2-C1E2-C1E1	116(1)	
C2E2-C2E1-N2	113(1)		C1E2-C1E1-N1	114(1)	
O2D1-C2D2-O2D2	126(1)		O1D1-C1D2-O1D2	128(1)	
O2D1-C2D2-C2D1	120.0(9)		O1D1-C1D2-C1D1	116(1)	
O2D2-C2D2-C2D1	113.9(9)		O1D2-C1D2-C1D1	115(1)	

Table 12. (Continued)

Atoms	Angles	Atoms	Angles
	Intraligand angles cont.		
C2D2-C2D1-N2	109.9(8)	C1D2-C1D1-N1	112(1)
O2U1-C2U2-O2U2	123(1)	O1U1-C1U2-O1U2	126(1)
O2U1-C2U2-C2U1	120(1)	O1U1-C1U2-C1U1	118(1)
O2U2-C2U2-C2U1	117(1)	O1U2-C1U2-C1U1	116(1)
C2U2-C2U1-N2	114.6(9)	C1U2-C1U1-N1	112(1)
C2E1-N2-C2D1	109.3(9)	C1E1-N1-C1D1	110(1)
C2E1-N2-C2U1	110.6(9)	C1E1-N1-C1U1	109(1)
C2D1-N2-C2U1	110.8(8)	C1D1-N1-C1U1	108(1)
	Angles involving a metal atom		
N2-Dy2-OW21	119.1(3)	OW11-Dy1-O1U1	141.1(4)
O2D1-Dy2-O2E1	102.8(3)	N1-Dy1-O1E1	68.2(3)
O2E2-Dy2-OW22	104.2(4)	O2D2-Dy1-O1E2	80.3(4)
O2U1-Dy2-O1D2	136.4(4)	O1D1-Dy1-OW12	156.3(3)
N2-Dy2-O1D2	134.3(2)	O2D2-Dy1-O1E1	130.9(3)
O2D1-Dy2-O2E2	79.1(3)	OW11-Dy1-OW12	98.8(4)
O2E1-Dy2-OW22	89.8(4)	N1-Dy1-O1E2	101.2(3)
OW21-Dy2-O2U1	135.2(4)	O1D1-Dy1-O1U1	116.9(3)
O2E2-Dy2-O2E1	140.9(3)	O1U1-Dy1-O1E1	72.3(4)
OW22-Dy2-O2D1	155.5(3)	O1D1-Dy1-O2D2	75.1(3)
N2-Dy2-O2U1	68.3(3)	OW12-Dy1-N1	137.1(3)
OW21-Dy2-O1D2	73.2(3)	O1E2-Dy1-OW11	146.4(4)

Table 12. (Continued)

Atoms	Angles	Atoms	Angles
Angles involving a metal atom cont.			
C2U2-O2U1-Dy2	125.0(8)	C1U2-O1U1-Dy1	118.9(9)
C2E2-O2E1-Dy2	123.0(8)	C1E2-O1E1-Dy1	124.5(8)
C2E2-O2E2-Dy2 <sup>b</sup>	159(1)	C1E2-O1E2-Dy2 <sup>b</sup>	164(1)
C2D2-O2D2-Dy2	121.5(7)	C1E2-O1D1-Dy1	128.7(7)
C2D2-O2D1-Dy1	134.0(8)	C1D2-O1D2-Dy2 <sup>b</sup>	128.7(7)
Atoms	Distance	Atoms	Distance
Additional interatomic distances			
O1E1-O1E2	2.18(1)	OW13-O1U2	2.89(2)
O2E1-O2E2	2.24(1)	OW14-OW11	2.59(2)
O1D1-O1D2	2.23(1)	OW14-O1U2	3.06(2)
O2D1-O2D2	2.21(1)	OW23-O2U2	2.69(2)
O1U1-O1U2	2.20(1)	OW23-OW12	2.85(1)
O2U1-O2U2	2.17(1)	OW24-O2U2	2.71(2)
OW13-OW11	2.78(2)	OW23-OW21	2.64(2)

<sup>b</sup>For an explanation of symmetry related positions see Figures 15 and 16.

Figure 14. Configuration of the two independent molecules. (The two metal atoms are numbered for uniqueness. The nitrogen atoms have the same number as the metal to which they are coordinated which is also the left-most number for the remaining atoms in the ligand. The letters specify the type of metal-oxygen coordination (see text), while the right-most number indicates a skeletal position for the carbon atoms. In the case of the oxygen atoms, a one in the right-most position indicates coordination to the same metal atoms as the nitrogen atom while a two indicates a different interaction)



(D type), and one is not coordinated to any metal atom (U type). Schematic drawings of the two independent NTA ligands are shown in Figures 15 and 16. The acetate groups are all planar to within  $0.03 \text{ \AA}$ ; the  $\text{O}_a\text{-C-O}_a$  angles average  $126^\circ$  ( $123\text{-}128^\circ$ ) while the  $\text{O}_a\text{-C-C}$  angles average  $117^\circ$  ( $114\text{-}120^\circ$ ). The average carbon-oxygen ( $1.26 \text{ \AA}$ ), carbon-carbon ( $1.55 \text{ \AA}$ ) and carbon-nitrogen ( $1.48 \text{ \AA}$ ) bond distances, corrected for thermal motion are all within  $0.01 \text{ \AA}$  of the expected values.<sup>39</sup>

The variation in C-C and C-N bond distances does not appear to be significant. The systematically large  $\text{O}_a\text{-C-O}_a$  angles are apparently the result of intermolecular steric interactions and intracarboxylate oxygen-oxygen repulsions.<sup>25</sup> Also, the wide range in metal-oxygen and C- $\text{O}_a$  distances probably is a result of a combination of steric and electrostatic effects. There does not appear to be any correlation between lengthenings and shortenings of C-O distances in a manner which would suggest covalent effects. In addition, the C- $\text{O}_a$  distance for the two uncoordinated oxygens are  $0.01 \text{ \AA}$  longer than the average; a shortening of this bond would be expected in the presence of covalent bonding.<sup>44</sup>

Five acetate oxygen atoms, two water molecules and one nitrogen atom are in the coordination sphere of each metal atom. These coordinating atoms reside at the corners of a distorted dodecahedron with triangular faces with approximate

Figure 15. Schematic drawing of NTA ligand one

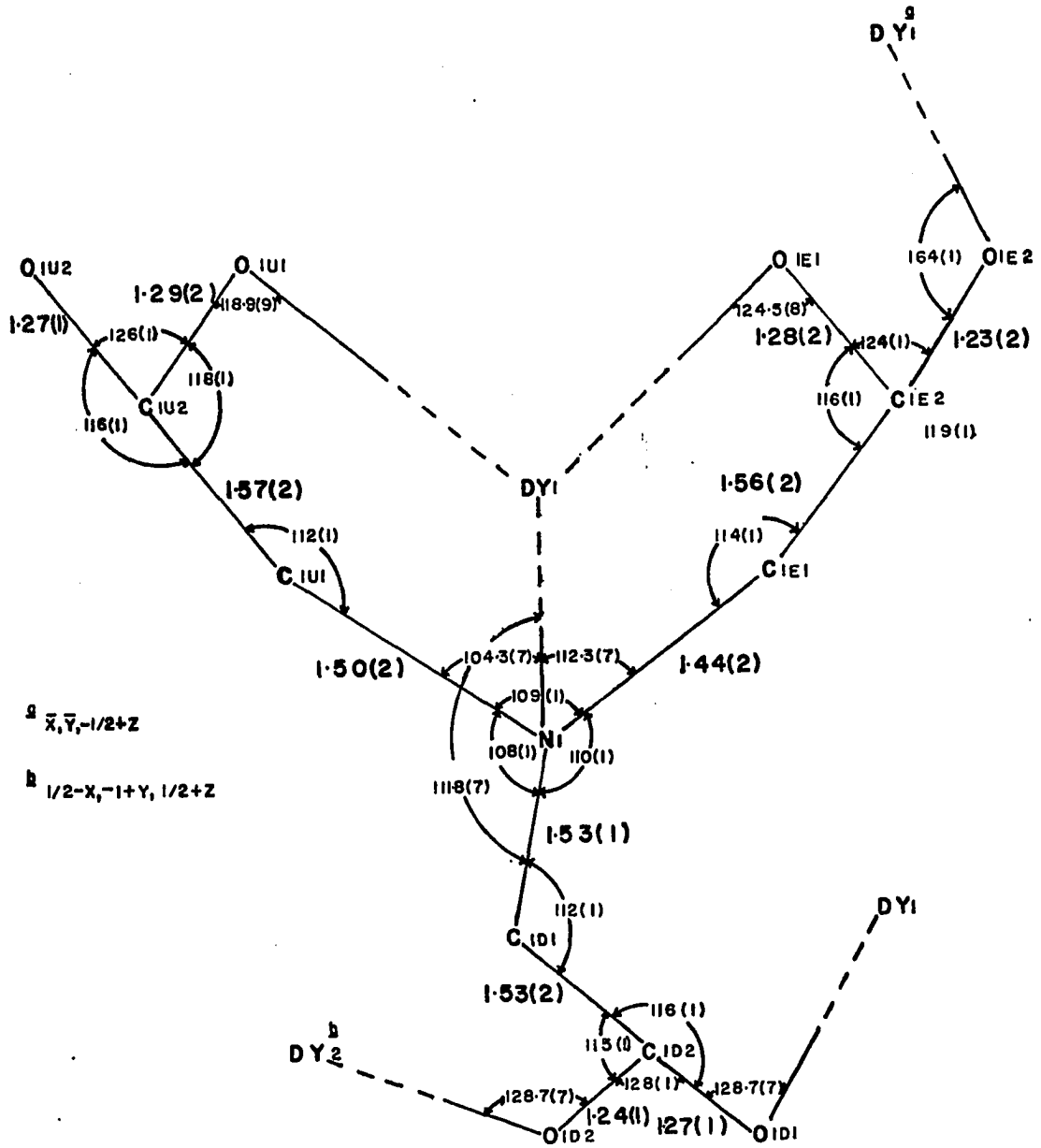
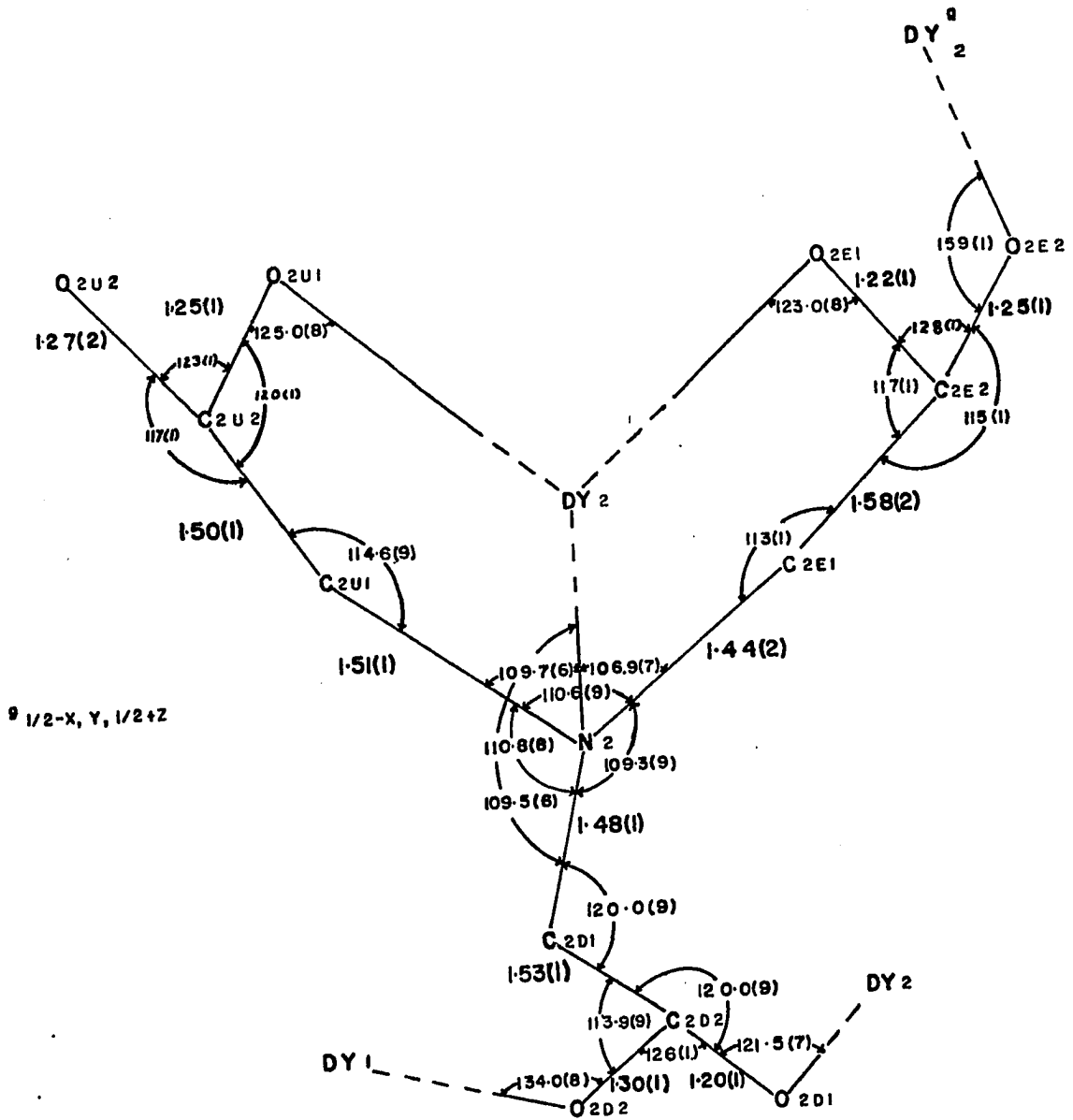




Figure 16. Schematic drawing of NTA ligand two



$D_{2d}$  symmetry. A projection down one of the two folds in molecule one and a projection showing the fourfold inversion axis in molecule two are given in Figures 17 and 18. The good agreement, in most cases, between symmetry equivalent distances (see Table 13) illustrates the approximate  $D_{2d}$  symmetry. The nona-coordinate, capped, square antiprism found in the  $\text{Pr}\cdot\text{NTA}\cdot 3\text{H}_2\text{O}$  can be converted to the octa-coordinate dodecahedron by removal of the atom in the capping position and relatively minor changes in angles. The NTA ligand in the Pr complex would then be hexadentate as it is in the title compound with no doubly coordinated oxygen atom.

The coordination can also be described as a distorted one-five-two complex similar to the one-five-three description given by Hoard *et al.*<sup>41</sup> for the  $\text{La}\cdot\text{EDTA}$  complex. The distortions are much greater in this case than for the dodecahedron and we prefer the latter.

The average  $\text{Dy}-\text{O}_a$ ,  $\text{Dy}-\text{N}$  and  $\text{Dy}-\text{O}_w$  distances, uncorrected for thermal motion are 2.346, 2.578, and 2.359 Å. This corresponds to a decrease of approximately 0.1 Å compared to the corresponding praseodymium distances for the  $\text{M}-\text{O}_a$  and  $\text{M}-\text{N}$  bonds. This is in good agreement with the decrease in the ionic radius.<sup>40</sup> The  $\text{Dy}-\text{O}_w$  distances average approximately 0.06 Å shorter than expected. However, there are a large number of  $\text{O}_w-\text{O}$  distances which are in the range typical of

Figure 17. Coordination of  $Dy_1$  (viewed down a pseudo, twofold axis)

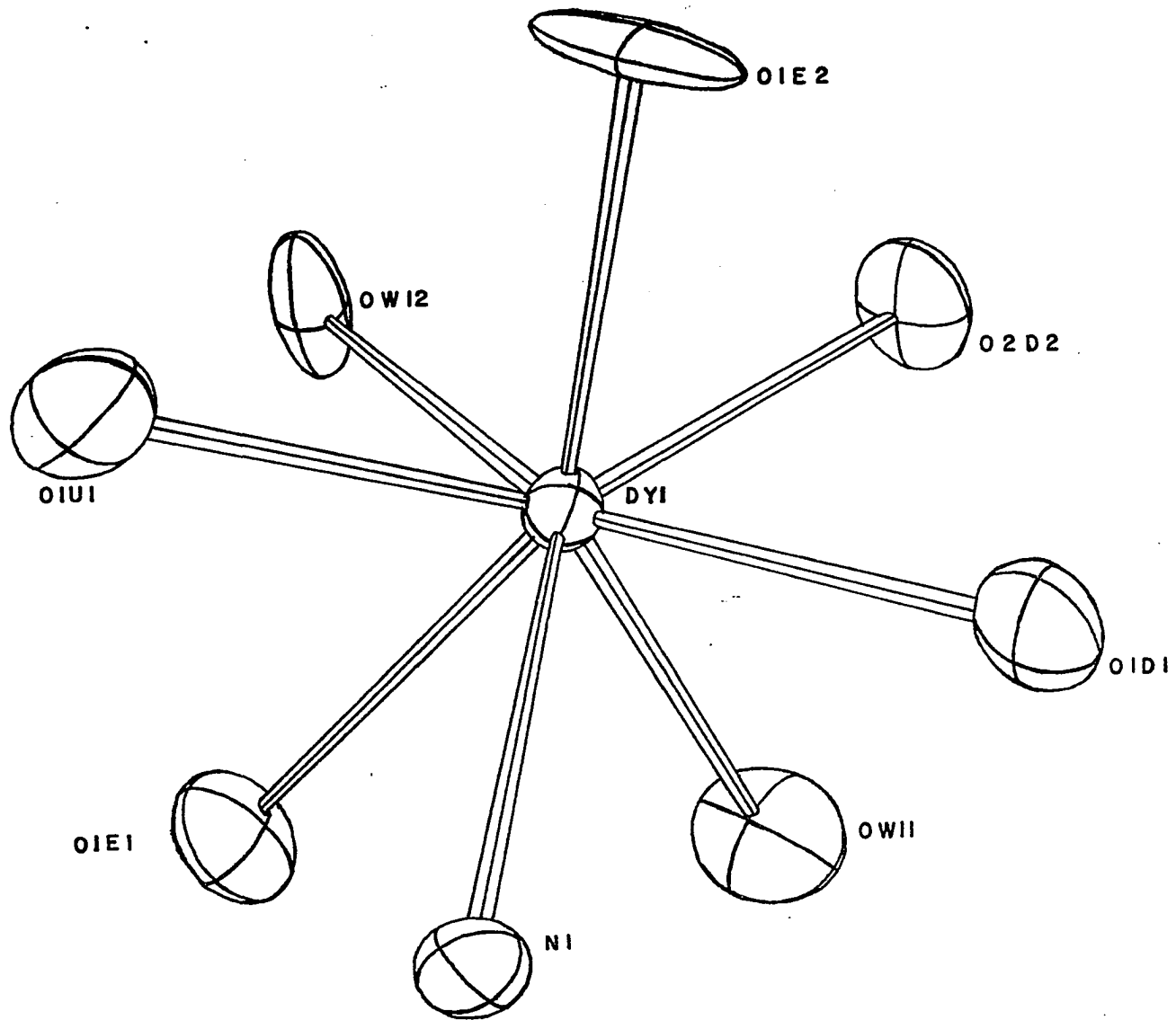


Figure 18. Coordination of  $Dy_2$  (viewed perpendicular to a pseudo,  $\bar{4}$  axis)

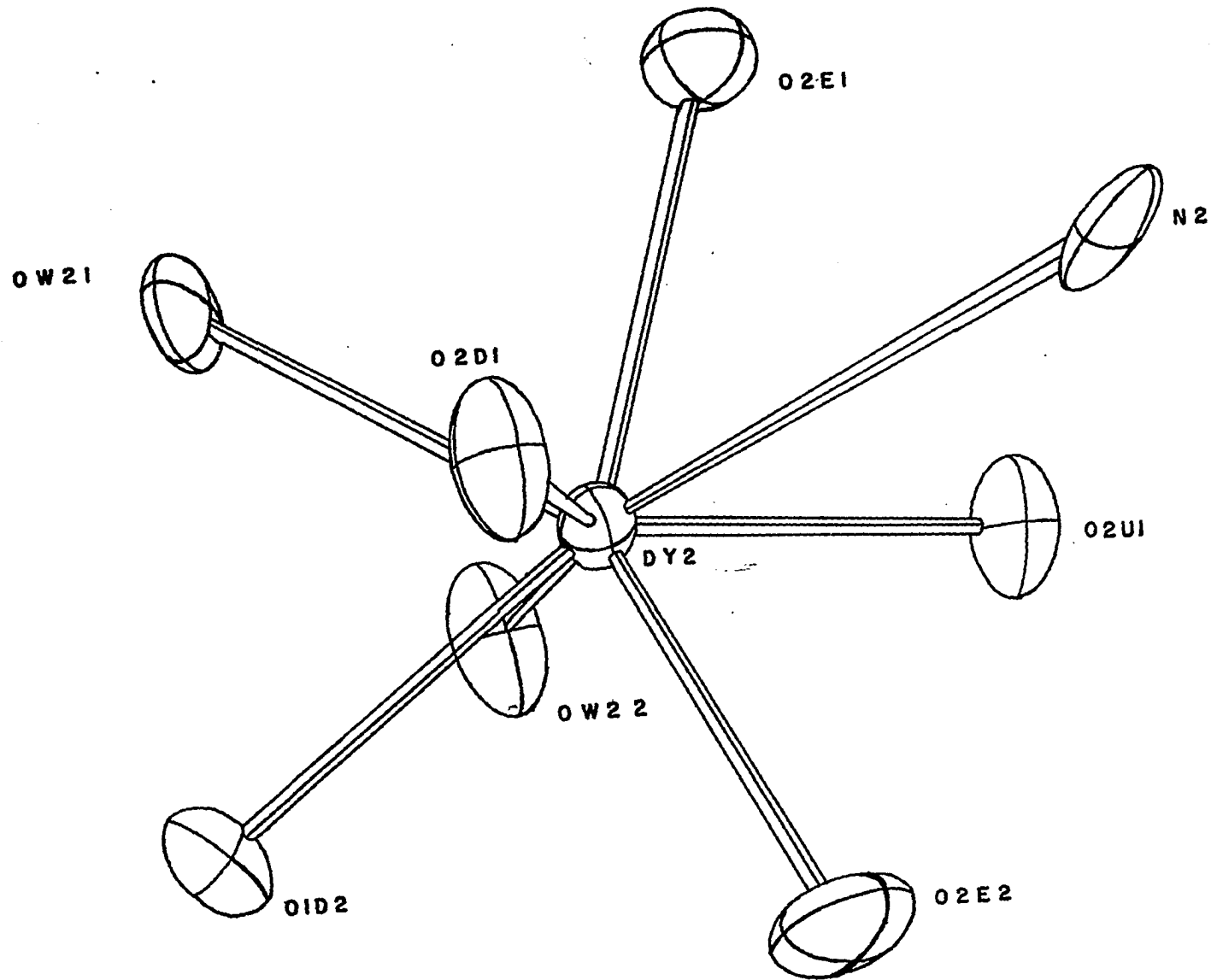


Table 13. Atoms and distances<sup>a</sup> related by pseudo-symmetry

Atoms related by a twofold					
Molecule 1			Molecule 2		
N1-O1E1	O2D2-O1E1		N2-OW21	OW21-O2U1	
OW11-O1U1	OW11-OW12		O1D2-O2U1	O2D1-O2E2	
O2D2-O1E2	N1-O1E2		O2D1-O2E1	N2-O1D2	
O1D1-OW12	O1D1-O1U1		O2E2-OW22	O2E1-OW22	
Atoms related by $\bar{4}$					
O1U1-O1D1-O1E1-O2D2			O2E2-OW22-O2E1-O2D1		
OW12-O1E2-N1-OW11			N2-OW21-O2U1-O1D2		
Equivalent distances related by pseudo-symmetry					
Molecule 1			Molecule 2		
Atoms	Dist.	Ave.	Atoms	Dist.	Ave.
O1E1-O1U1	2.78		O1D2-OW21	2.85	
		2.80			2.81
O1D1-O2D2	2.83		O2U1-N2	2.77	
O1E1-N1	2.77		O1D2-O2D1	2.85	
O1D1-O1E2	2.85		OW21-OW22	3.05	
O1U1-OW12	3.06		N2-O2E1	2.78	
O2D2-OW11	2.78		O2E2-O2U1	2.87	
		2.88			2.97
O1E1-OW12	2.87		O1D2-OW22	3.19	
O1E1-N1	2.77		OW21-O2D1	3.11	

<sup>a</sup>Average standard deviation in distances is 0.02 Å.



Table 13. (Continued)

Atoms	Dist.	Ave.	Atoms	Dist.	Ave.
O1D1-OW11	2.95		N2-02E2	3.09	
O2D2-01E2	2.98		O2U1-02E1	2.85	
N1-01E2	3.76		O2D1-02E1	3.69	
OW11-OW12	3.60		O2D1-02E2	2.95	
		3.57			3.41
N1-OW11	3.47		OW22-02E1	3.34	
OW12-01E2	3.44		OW22-02E2	3.67	
O1E1-OW11	2.70		O1D2-02E2	2.89	
O1U1-01E2	2.72		OW21-02E1	2.94	
		2.80			2.77
O1D1-N1	2.69		N2-02D1	2.67	
O2D2-OW12	3.08		O2U1-OW22	2.78	

hydrogen bonding (Tables 12 and 13) and such hydrogen bonding might be expected to increase the metal- $O_w$  interactions on electrostatic grounds.

## THE QUADRUPLE PRODUCT

## Introduction

The basis for the method to be described below as well as for any of the so called "direct methods" is the Sayre<sup>52</sup> squared equation

$$V \times S \times \underline{F}_{\underline{h}} = \sum_{\underline{k}} \underline{F}_{\underline{k}} \underline{F}_{\underline{h}-\underline{k}} \quad (1)$$

where  $V$  is the volume of the unit cell and  $S$  is a function to correct for a difference in peak-shape between  $\underline{F}_{\underline{h}}$  and  $\underline{F}_{\underline{h}-\underline{k}}$ . This function is a direct result of the self-convolution of the structure factor,  $\underline{F}_{\underline{h}}$ .<sup>53</sup> It is apparent for centrosymmetric space groups, where phases are limited to integral values ( $\pm 1$ ), that in order for  $\underline{F}_{\underline{h}}$  to be large, the values within the summation must tend strongly towards terms with the same sign. Therefore, for most terms in Equation 1,

$$s(\underline{F}_{\underline{h}}) = s(\underline{F}_{\underline{k}})s(\underline{F}_{\underline{h}-\underline{k}}) \quad (2)$$

where  $s$  represents "the sign of". The larger the values of  $\underline{F}_{\underline{h}}$ ,  $\underline{F}_{\underline{k}}$ , and  $\underline{F}_{\underline{h}-\underline{k}}$ , the more probable that (2) will hold. A more useful measure of a particular reflections "largeness" is its  $\underline{E}$  value.<sup>54</sup> This is simply the value of  $\underline{F}$  corrected for  $\sin\theta/\lambda$  fall-off in the scattering power

$$\frac{\underline{E}_{\underline{h}}^2}{h} = \frac{\underline{F}_{\underline{h}}^2}{h} / \epsilon \sum_j^N f_j^2 \quad (3)$$

where  $f_j$  is the scattering factor,  $\underline{\epsilon}$  is a term which is introduced to correct for symmetry, and  $\underline{F}_{\underline{h}}$  is corrected for thermal motion. The use of  $\underline{E}_{\underline{h}}$  instead of  $\underline{F}_{\underline{h}}$  makes possible meaningful size comparisons between reflections at different values of  $\theta$ . When the size of a particular reflection is expressed in terms of  $\underline{E}_{\underline{h}}$ 's, then the probability that (2) will hold is given by<sup>55</sup>

$$P(+)=1/2+1/2 \tanh \rho_3/\rho_2^{3/2} \left| \frac{\underline{E}_{\underline{h}-\underline{k}} \underline{E}_{\underline{h}-\underline{k}}}{\underline{E}_{\underline{h}} \underline{E}_{\underline{k}}} \right| \quad (4)$$

where  $\rho_q = \sum_i^N n_i^q$  and  $n_i = f_i / \sum_j^N f_j$ . If there are multiple relations which yield  $\underline{E}_{\underline{h}}$ , then

$$P(+)=1/2+1/2 \tanh \sum_k \rho_3/\rho_2^{3/2} \left| \frac{\underline{E}_{\underline{h}-\underline{k}} \underline{E}_{\underline{h}-\underline{k}}}{\underline{E}_{\underline{h}} \underline{E}_{\underline{k}}} \right| \quad (5)$$

The normal manner in which the signs of the various reflections are determined in a centrosymmetric structure is to use a "symbolic addition procedure".<sup>56-59</sup> In this procedure initial signs are given to a few reflections (three or less) with larger values of  $\underline{E}$  to fix the origin and additional algebraic symbols are given to a few other reflections as needed. By the application of Equation (2), additional signs may be determined. Failure in this method usually is a result of either poor data, difficulty in choosing a good starting set, or few type (2) relationships with high probability. The last case is especially important in triclinic systems because of the low symmetry. In the method

described below, an attempt was made to develop additional phase relationships between the various reflections. In this manner, the dependency of the solution upon the choice of a good starting set can be eliminated and the problems caused by only a few type (2) relationships may be reduced.

#### Description of the Method

When  $\underline{E}_{\vec{h}}$  is large, all the individual signs of the terms in Equation (1) are equated; this results in a series of equations of the type

$$s(\underline{E}_{\vec{k}})s(\underline{E}_{\vec{h}-\vec{k}}) = s(\underline{E}_{\vec{k}'})s(\underline{E}_{\vec{h}-\vec{k}'}) \quad (6)$$

for all possible values of  $\vec{k}$  and  $\vec{k}'$ ,  $\vec{k} \neq \vec{k}'$ . The probability that these equations hold is just the product of the probabilities that each individual relation of the type (2) holds. Upon rearrangement of (6)

$$s(\underline{E}_{\vec{k}})s(\underline{E}_{\vec{h}-\vec{k}})s(\underline{E}_{\vec{k}'})s(\underline{E}_{\vec{h}-\vec{k}'}) = +1 \quad (7)$$

is obtained. This relationship we have chosen to call the quadruple product. In every centrosymmetric structure there will be at least one set, and sometimes several sets, depending upon the amount of symmetry present, of  $\vec{h}$ ,  $\vec{k}$ ,  $\vec{k}'$  values where two of the unknowns can be eliminated from Equation(7). For example, two sets of  $\underline{E}$ 's which satisfy Equation (2) for a value of  $\vec{h} = 1, 3, 3$  are  $\underline{E}_{111} \cdot \underline{E}_{022}$  and

$\underline{E}_{111} \cdot \underline{E}_{244}$ . These two sets would then give rise to the quadruple product

$$s(\underline{E}_{111}) \cdot s(\underline{E}_{022}) \cdot s(\underline{E}_{111}) \cdot s(\underline{E}_{244}) = +1 \quad (8)$$

For a centrosymmetric structure  $\underline{E}_{111} = \underline{E}_{111}$  and

$$s(\underline{E}_{111}) \cdot s(\underline{E}_{111}) = +1 \quad (9)$$

Upon substitution of Equation (9) into Equation (8)

$$s(\underline{E}_{022}) \cdot s(\underline{E}_{244}) \cdot (+1) = +1 \quad (10)$$

is obtained, or, upon rearrangement

$$s(\underline{E}_{022}) = s(\underline{E}_{244}) \quad (11)$$

The probability that the relationship given by Equation (11) holds is the same as that of the parent quadruple relation holding.

As soon as the relationship between two  $\underline{E}_h$ 's is known with high probability ( $\sim 0.95$ ), then this relation can be fed back into the sign determining process and the number of quadruple products, from which two unknowns can be eliminated, rapidly increases. The probability that these new relationships will hold is just equal to the product of the probabilities that the quadruple product holds and the relation between the two  $\underline{E}_h$ 's, which are eliminated, is valid. Since this new probability is the product of four numbers all less

than one, it is apparent that a single relationship may well have a probability which is small ( $\ll 0.95$ ). However, as the number of relationships between  $\underline{E}_h$ 's increases, so will the number of multiple indications of a particular relationship between two  $\underline{E}$ 's. For two indications, the probability that an indication is correct is

$$P(c) = P_1 \times P_2 / (1 - P_1 - P_2 + 2P_1 \times P_2) \quad (12)$$

where  $P_1$  and  $P_2$  are the probabilities of the individual relationships being valid. In general, for  $n$  indications the probability can be expressed as

$$P(c) = \frac{\prod_{i=1}^n P_i}{\prod_{i=1}^n (1 - P_i) + \prod_{i=1}^n (P_i)} \quad (13)$$

It is apparent that with only a few indications of moderate probability ( $\sim 0.8$ ), Equation (13) will rapidly approach unity.

A particular reflection may be placed in any one of eight parity groups: eee, eeo, eoe, oee, eoo, oeo, ooe, and ooo where e indicates even and o indicates an odd index. The parties are seen to form a group with respect to multiplication (Table 14). It is readily seen that, in order to satisfy Equation (2) for a given parity of  $\vec{h}$ ,  $\underline{E}$ 's of appropriate parity must be used. For example, if  $\vec{h}$  has parity eoe, there will be four combinations of two  $\underline{E}$ 's which will yield this parity (oeo, ooo; eee, eoe; ooe, oee;

Table 14. Parity group multiplication table

	eee	eeo	eeo	oee	ooe	oeo	eoo	ooo
eee	eee	eeo	eeo	oee	ooe	oeo	eoo	ooo
eeo	eeo	eee	eoo	oeo	ooo	oee	eeo	oee
eeo	eeo	eoo	eee	oee	oee	ooo	eeo	oeo
oee	oee	oeo	oee	eee	eeo	eeo	ooo	eoo
ooe	ooe	ooo	oee	eeo	eee	eoo	oeo	eeo
oeo	oeo	oee	ooo	eeo	eoo	eee	oee	eeo
eoo	eoo	eeo	eeo	ooo	oeo	oee	eee	oee
ooo	ooo	oee	oeo	eoo	eeo	eeo	oee	eee

eeo, eoo). In addition, if two of the three parity groups are specified then, obviously, the parity of the third term is determined. This is important since it dictates that only terms of like parity may be related through Equation (11) before the origin is defined.

When relationships within the various parity groups are known, the origin may be specified. Using the known intra-parity relationships, absolute signs may be assigned to the E's in the parity groups of the origin defining E's. Since there are now many new relationships between E's in the different parity groups, there will be many additional quadruple products where two of the unknowns, now of dif-



ferent parity classes, may be eliminated.

Absolute signs may be determined for the remaining parity groups by two different procedures. The first procedure is to make use of type (2) relationships. When two  $\underline{E}_{\vec{h}}$ 's have known absolute signs and the third  $\underline{E}_{\vec{h}}$  is of a parity class for which absolute signs are not known, the absolute signs of the third parity group can be obtained. For example, the necessary relationships needed to relate relative signs of the undetermined parity groups to those of the three parity groups eee, oee, eoe are shown in Table 15.

Table 15. Parities which relate relative signs

	$\vec{h}$	$\vec{k}$	$\vec{h}-\vec{k}$
	ooo	ooo	ooo
	ooe	oee	oee
	oeo	oee	eeo
	eoo	oee	eeo
Cycle 1	eee	oee	oee
	eee	oee	oee
	eee	oee	oee
	eee	oee	oee
	eee	oee	oee
Cycle 2	ooo	ooo	ooo

In order to determine the ooo parity group, it would be necessary to recycle using relative signs generated in the first cycle. The probability that these new signs are

correct would be the probability that Equation (2) holds, times the probability that the relationship between the two known  $\underline{E}_H$ 's, as determined from the quadruple product, is valid. Only relationships of very high probability ( $\sim 0.99$ ) need be used in this process since there will be numerous indications for the absolute signs of each of the unknown groups and these probabilities will rapidly approach certainty by the use of equations similar to (13).

The second procedure, which can be used to determine the absolute signs of the unknown parity classes, utilizes the absolute signs of the eee-type reflections which can be determined before the origin is defined. When two  $\underline{E}$ 's with the same parity are involved in a type 2 relation, the parity of the third  $\underline{E}$  must be eee. If the  $\underline{E}$ 's are of the same parity, their relative signs will be known and Equation (2) can be uniquely solved for the absolute sign of the eee- $\underline{E}$ . There are usually a number of these types of relations for every eee- $\underline{E}$  and the associated probabilities will approach certainty by the use of equations similar to (13). After the origin is defined, there are a number of quadruple products which involve two  $\underline{E}_H$ 's of a parity class with known absolute signs, an  $\underline{E}_H$  of eee parity with known absolute sign, and one  $\underline{E}_H$  from an unknown parity group. The absolute sign for this  $\underline{E}_H$  is then uniquely determined. The types of parities needed to relate the absolute signs of the undeter-

mined parity groups to the three parity groups  $eeo$ ,  $oeo$ ,  $ooo$  by the use of the quadruple product and known signs for the  $eee$ - $E$ 's are shown in Table 16. The quadruple products are, of course, formed with  $\vec{k}$  and  $\vec{h}-\vec{k}$  terms. It is also seen in

Table 16. Types of parities needed to relate undetermine signs

$\vec{h}$	$\vec{k}$	$\vec{h}-\vec{k}$	$\vec{h}$	$\vec{k}$	$\vec{h}-\vec{k}$	$\vec{h}$	$\vec{k}$	$\vec{h}-\vec{k}$
	$oeo$	$oeo$		$oeo$	$oeo$		$oeo$	$ooo$
$eeo$	$oeo$	$ooo$	$oeo$	$oeo$	$ooo$	$oeo$	$oeo$	$ooo$
	$ooo$	$ooo$		$ooo$	$ooo$		$ooo$	$ooo$
$ooo$	$oeo$	$ooo$	$ooo$	$oeo$	$ooo$	$ooo$	$oeo$	$ooo$
	$oeo$	$ooo$		$oeo$	$ooo$		$oeo$	$ooo$

Table 16 that the absolute signs of one of the parity groups (in this case the  $ooo$  type) is determined directly from the origin defining parity groups.

In practice a mixture of the two methods described above is used. The second method is routinely used in an automated procedure since it is easier to program and, in addition, it leads to new relationships between  $E_{\vec{h}}$ 's which are not found through symmetry alone. The first procedure is used only if

the automated procedure fails. This only occurs when there are a small number of E's in a particular parity group or when small sub-groups form where a few of the E's have no interrelations with the bulk of the E's in a particular parity group. In these cases the (2)-type relationships may be used to find the unknown signs.

#### Application of the Method

To facilitate the application of this method two programs, Quads and Relate have been written. The calculation of the quadruple products is carried out by the use of the program Quads. A listing of this Fortron IV program is supplied in Appendix A. Input to this program is a tape containing all relations of the type (2). The actual sign determination process is carried out using Relate. Relate is a PL-1 program written for the 360-65 system. It uses 22K words of high speed core with some dynamic allocation of arrays plus an additional 50K words of slow core. A listing of this program can be found in Appendix B.

Relate searches through the entire list of quadruple products for relationships where the relative signs of two of the four members are known. The remaining two members are then given the appropriate relative sign and the probability is stored, or if there is already some indication known between these E<sub>h</sub>'s, a new probability is calculated. At the end of each cycle, the probabilities are searched for values

exceeding a cut-off value ( $\sim 0.95$ ). These relationships are then output along with their associated probabilities. This list of related  $\underline{E}_h$ 's is then searched for relationships of the type  $a = \pm b$  and  $b = \pm c$ . Then  $a$  is set equal to  $c$  with the appropriate relative sign. Finally, the list of relationships of type (2) involving eee reflections is searched for cases where two of the three unknowns may be eliminated. If the cumulated probability exceeds a given cut-off value ( $\sim 0.99$ ), the  $\underline{E}_h$ , where  $h$  is eee, is given the appropriate absolute sign. Then if any of the type (2) relations which contain this  $s(\underline{E}_h)$  are not known, the remaining two members are given the appropriate relative sign and probabilities. The program then recycles using these newly determined relations. Whenever most of the relations for the various parity groups are known, the origin is defined by assigning absolute signs to appropriate reflections. The program then recycles through the type (2) relations and determines the signs of the remaining groups. It also continues to cycle through the quadruples since in so doing the signs of some previously undetermined  $\underline{E}_h$ 's may be found.

The method has been tested on the structure of  $\text{Cs}_3\text{Sb}_2\text{Cl}_9$  which crystallizes in the space group Pnma (No. 62) with  $Z = 4$ . This structure was previously solved by W. Pflaum using normal direct methods. Values of the  $\underline{E}$ 's were calculated using a scale factor of 0.20 and an overall thermal parameter

of 2.65 determined by the method of Hackert.<sup>60</sup> The relations of type (2) were calculated<sup>8</sup> for  $E_h$ 's above 1.5. The value of  $\rho_3/\rho_2^{3/2}$  used in calculating the probabilities was 0.143. Due to the limited core size of 50K words, only the 196  $E_h$ 's above 2.28 were used in the calculation of some 62,560 quadruple products. In Relate, quadruple products were accepted only if their probability exceeded 0.80. A relationship between two  $E_h$ 's had to exceed a probability of 0.95 before it was accepted. Before signs were accepted for groups of reflections or for eee type reflections, the associated probability had to exceed 0.99. After three cycles through Relate, absolute signs were given appropriate members of the oee, ooe and eoo parity groups. In this case, all signs of the remaining groups were obtained automatically. Of the 196 inputs  $E_h$ 's, 194 were successfully assigned signs. Of these 194 signs, all were correct. From an E-map using these signs the positions of the Cs and Sb atoms were readily located. In Table 17 are listed the hkl values, and the signed  $E_h$  values.



Table 17. (Continued)

---

4	0	8	3.93	8	2	10	3.38	15	0	14	-2.70	24	2	2	2.30
4	0	10	-2.40	8	2	14	3.05	15	1	1	2.30				
4	0	16	2.65	8	3	1	2.57	15	1	7	-2.30				
4	2	2	3.65	8	3	5	2.29	15	1	13	2.50				

---



## LITERATURE CITED

1. Brockway, L. O. and J. Y. Beach, J. Am. Chem. Soc., 60, 1836 (1938).
2. Brockway, L. O. and N. R. Davidson, J. Am. Chem. Soc., 63, 3287 (1941).
3. Takano, T., N. Kasai, and M. Kakudo, Bull. Chem. Soc. Japan, 36, 585 (1963).
4. Gilman, H., R. L. Harrell, C. L. Smith, and K. Shiina, J. Organometallic Chem., 5, 387 (1966).
5. Williams, D. E. and R. E. Rundle, J. Am. Chem. Soc., 86, 1660 (1964).
6. Busing, W. R., K. O. Martin, and H. A. Levy, U.S. Atomic Energy Commission Report ORNL-TM-305 [Oak Ridge National Laboratory, Tenn.], 1959.
7. Ahmed, F. R., S. R. Hall, M. E. Pippy, and C. P. Saunderson, "NRC Crystallographic Programs for the IBM/360 System", National Research Council of Canada Report [Ottawa, Canada], 1968.
8. Hanson, H. P., F. Herman, J. D. Lea, and S. Skillman, Acta Cryst., 17, 1040 (1964).
9. Hamilton, W. C., Acta Cryst., 18, 502 (1965).
10. Johnson, C. K., U.S. Atomic Energy Commission Report ORNL-3799-uc-4 [Oak Ridge National Laboratory, Tenn.], 1965.
11. Harrell, R. L., Ph.D. Thesis, Iowa State University, Ames, Iowa, 1966.
12. Gilman, H., W. H. Atwell, P. K. Sen, and C. L. Smith, J. Organometallic Chem., 4, 163 (1965).
13. Hague, D. N. and R. H. Prince, J. Chem. Soc., 4690 (1965).
14. Gilman, H. and D. R. Chapman, J. Organometallic Chem., 5, 392 (1966).
15. Higuchi, T. and A. Shimada, Bull. Chem. Soc. Japan, 39, 1316 (1966).

16. Weyenberg, D. R. and L. H. Toporger, J. Am. Chem. Soc., 84, 2843 (1962).
17. Straumanis, M. E. and E. Z. Aka, J. Appl. Phys., 23, 330 (1952).
18. Booth, G., Advances in Inorganic Chemistry and Radiochemistry, 6, 37 (1964).
19. Coates, G. E. and C. Parkin, J. Chem. Soc., 421 (1963).
20. Keiter, R., Ph.D. Thesis, University of Maryland, College Park, Maryland, 1966.
21. Bailey, N. A. and R. Mason, J. Chem. Soc., 2594 (1968).
22. "International Tables of X-ray Crystallography", Vol. III, Kynoch Press, Birmingham, England, 1965.
23. Busing, W. R., K. O. Martin, and H. A. Levy, U.S. Atomic Energy Commission Report ORNL-TM-306 [Oak Ridge National Laboratory, Tenn.], 1964.
24. Pauling, L., "The Nature of the Chemical Bond", 3rd ed., Cornell University Press, Ithaca, N.Y., 1960.
25. Bartell, L. S., J. Chem. Phys., 32, 827 (1960).
26. Bennett, M. J., F. A. Cotton, and D. L. Weaver, Acta Cryst., 23, 788 (1967).
27. Chatt, J., L. A. Duncanson, and L. W. Venanzi, J. Chem. Soc., 4456 (1955).
28. Messmer, G. G., E. L. Amma, and J. A. Ibers, Inorg. Chem., 6, 725 (1967).
29. Messmer, G. G. and E. L. Amma, Inorg. Chem., 5, 1775 (1966).
30. Fitch, F. T. and D. S. Russel, Can. J. Chem. Soc., 29, 363 (1951).
31. Levy, S. C. and J. E. Powell, U.S. Atomic Energy Commission Report IS-421 [Ames Laboratory, Iowa], 1961.
32. Moeller, T., E. R. Birnbaum, J. H. Forsberg and R. B. Gaghart, Prog. in the Science and Tech. of the Rare Earths, 3, 61 (1968).

33. Templeton, D. H. and G. F. Cater, J. Phys. Chem., 58, 940 (1954).
34. Zalkin, A., D. H. Templeton and D. G. Karraker, Inorg. Chem., 8, 2680 (1969).
35. Urgo, J. F., Ph.D. Thesis, Iowa State University, Ames, Iowa, 1968.
36. Lind, M. D., B. Lee, and J. L. Hoard, J. Am. Chem. Soc., 87, 1611 (1965).
37. Cromer, D. T. and J. T. Waber, Acta Cryst., 18, 104 (1965).
38. "Tables of Interatomic Distances", Special Publication No. 11, The Chemical Society of London, London, England, 1958.
39. "Tables of Interatomic Distances, Supplement", Special Publication No. 18, The Chemical Society of London, London, England, 1965.
40. Templeton, D. H. and C. H. Danben, J. Am. Chem. Soc., 76, 5237 (1954).
41. Hoard, J. L., B. Lee, and M. D. Lind, J. Am. Chem. Soc., 76, 5237 (1965).
42. Muetterties, E. L. and C. M. Wright, Quart. Rev., 21, 109 (1967).
43. Morosin, B., J. Chem. Phys., 49, 3007 (1968).
44. Beineke, T. A. and J. DelGaudio, Inorg. Chem., 7, 715 (1968).
45. Watkins, E. D., J. A. Cunningham, T. Phillips, D. E. Sands, and W. F. Wagner, Inorg. Chem., 8, 29 (1969).
46. Marezio, M., H. A. Plettinger, and W. H. Zachariasen, Acta Cryst., 14, 234 (1961).
47. Helmholtz, L., J. Am. Chem. Soc., 61, 1544 (1939).
48. Rumanova, I. M., G. F. Volodine, and N. V. Belor, Kristallografiya, 9, 642 (1964).
49. Larsen, R. D. and G. H. Brown, J. Phys. Chem., 68, 3060 (1964).

50. Bueger, M. J., Acta Cryst., 3, 87 (1950).
51. Busing, W. R. and H. A. Levy, Acta Cryst., 17, 142 (1964).
52. Sayre, D., Acta Cryst., 5, 60 (1952).
53. Bockner, S. and K. Chandrasekharan, "Fourier Transforms", Princeton University Press, Princeton, New Jersey, 1949.
54. Karle, J. and H. Hauptmann, Acta Cryst., 9, 635 (1956).
55. Cochran, W. and M. M. Woolfson, Acta Cryst., 8, 1 (1955).
56. Karle, I. L., K. Britts and P. Gum, Acta Cryst., 17, 496 (1964).
57. Karle, I. L. and K. Karle, Acta Cryst., 16, 969 (1963).
58. Karle, I. L. and J. Karle, Acta Cryst., 17, 1356 (1964).
59. Hauptman, H. and J. Karle, "ACA Monograph No. 3", American Crystallographic Association, New York, New York, 1953.
60. Hackert, M. L., Ph.D. Thesis, Iowa State University, Ames, Iowa, concurrent.

## ACKNOWLEDGMENTS

The author wishes to express his gratitude to Dr. T. A. Beineke for his guidance in the early stages of this research. The author is especially grateful to Dr. R. A. Jacobson for his inspiration and advice throughout this research.

The author is also indebted to Mr. J. E. Benson and Mr. H. F. Hollenbeck for their assistance in the collection of data and to the members of X-ray groups I and II who provided the stimulating environment so necessary for the development of a Ph.D. aspirant.

Thanks go to Drs. H. Gilman, R. Keiter and J. E. Powell for supplying samples of the silicon, palladium, and rare earth compounds, respectively.

The author is especially indebted to his wife, Martha, whose patience and understanding aided him greatly throughout the last two years.

APPENDIX A. A LISTING OF QUADS

C	QUADS. IS A FORTRAN IV PROGRAM TO CALCULATE THE QUADRUPLE PRODUCTS	QUA 0010
C	AND THE ASSOCIATED PROBABILITIES.....INPUT TO THIS PROGRAM	QUA 0020
C	IS THREE TAPES AND ONE CARD.....INFORMATION SUPPLIED ON THE	QUA 0030
C	INPUT TAPE IS THE SAME AS THAT OUTPUT FROM NRC-SAP-2	QUA 0040
C	INFORMATION SUPPLIED BY THE USER ON CARDS IS AS FOLLOWS.....	QUA 0050
C	NTAP-SPECIFIES ON WHICH UNIT THE INPUT TAPE SHOULD BE MOUNTED	QUA 0060
C	IOTAP-SPECIFIES ON WHICH UNIT THE OUTPUT TAPE 1 SHOULD BE MOUNTED	QUA 0070
C	NOTAP-SPECIFIES ON WHICH UNIT THE OUTPUT TAPE 2 SHOULD BE MOUNTED	QUA 0080
C	AMIN-THE MINIMUM ACCEPTABLE PROBABILITY	QUA 0090
C	MH-MAXIMUM SERIAL NUMBER TO BE CONSIDERED IN EVEN PARITY SEARCH	QUA 0100
C	MK-MAXIMUM SERIAL NUMBER TO BE CONSIDERED	QUA 0110
C	ML-DUMMY VARIABLE	QUA 0120
C	SIGMA-VALUE OF SIGMA3/SIGMA2 TO THE 3/2 POWER	QUA 0130
C	FORMAT 3I10,F10.5,3I5,F10.5	QUA 0140
C	OUTPUT FROM PROGRAM IS AS FOLLOWS.....HKL VALUES FOR ALL E'S	QUA 0150
C	ALONG WITH AN INDICATOR FOR EEE PARITY	QUA 0160
C	ALL OF THE QUADRUPLE PRODUCTS	QUA 0170
C	THE TOTAL NUMBER OF QUADS CALCULATED	QUA 0180
C	THE MAGNETIC TAPES CONTAIN THE FOLLOWING INFORMATION.....	QUA 0190
C	TAPE 1 HAS ALL OF THE QUADRUPLE PRODUCTS AND THEIR ASSOCIATED	QUA 0200
C	PROBABILITIES.....	QUA 0210
C	TAPE 2 CONTAINS ALL THE EEE TRIPLES.....	QUA 0220
C	BOTH OF THESE TAPES WILL BE NEEDED REPEATEDLY.....	QUA 0230
	DIMENSION N1(200),N2(200),A(200),TITLE(20),NQ(24),NNA(12),NNB(12)	QUA 0240
	DIMENSION MMM(401),NNC(12),NND(12),SIGG(12)	QUA 0250
	IZ=0	QUA 0260
	II=0	QUA 0270
	IN=0	QUA 0280
C	INPUT INFORMATION.....	QUA 0290
	READ(1,100)TITLE	QUA 0300
100	FORMAT(20A4)	QUA 0310
	WRITE(3,101)TITLE	QUA 0320
101	FORMAT(1H ,20A4//)	QUA 0330
	READ(1,102)NTAP,IOTAP,NOTAP,AMIN,MH,MK,ML,SIGMA	QUA 0340
102	FORMAT(3I10,F10.5,3I5,F10.4)	QUA 0350
	ND=0	QUA 0360
	WRITE(3,1001)NTAP,IOTAP,AMIN	QUA 0370

1001	FORMAT(1H , 'INPUT TAPE IS', I5, 'OUTPUT TAPE IS', I5, 'AMIN IS', F10.3)	QUA 0380
C	CALCULATE PARITY.....	QUA 0390
8	READ(NTAP) IH, IK, IL	QUA 0400
	IF(IH.GE.99)GO TO 93	QUA 0410
	II=II+1	QUA 0420
	NH=(IH/2)*2	QUA 0430
	NK=(IK/2)*2	QUA 0440
	NL=(IL/2)*2	QUA 0450
	IF(NH.NE.IH)GO TO 90	QUA 0460
	IF(NK.NE.IK)GO TO 90	QUA 0470
	IF(NL.NE.IL)GO TO 90	QUA 0480
	MMM(II)=1.	QUA 0490
	GO TO 91	QUA 0500
90	MMM(II)=0	QUA 0510
91	WRITE(3,1003) II, IH, IK, IL, MMM(II)	QUA 0520
1003	FORMAT(1H , I5, 5X, 4I5)	QUA 0530
	GO TO 8	QUA 0540
93	READ(NTAP)	QUA 0550
	WRITE(3,1004)	QUA 0560
1004	FORMAT(1H , 'I AM HERE')	QUA 0570
5	I=0	QUA 0580
	IN=0	QUA 0590
6	READ(NTAP, END=60) NA, NB, ES, PS	QUA 0600
C	CALCULATE PROBABILITIES.....	QUA 0610
	VAL=ABS(ES)	QUA 0620
	ARG=SIGMA*VAL	QUA 0630
	PROB=0.5+0.5*TANH(ARG)	QUA 0640
	PROB=PROB*VAL/ES	QUA 0650
	IF(NA)20,20,7	QUA 0660
7	IF(NA.GT.MH)GO TO 6	QUA 0670
	IF(NB.GT.MH)GO TO 6	QUA 0680
	IZ=IZ+1	QUA 0690
	NNA(IZ)=NA	QUA 0700
	NNB(IZ)=NB	QUA 0710
	SIGG(IZ)=PROB	QUA 0720
	IF(IZ.LT.8)GO TO 23	QUA 0730
	WRITE(3,1006)(NNA(N),NNB(N),SIGG(N),N=1,8)	QUA 0740



1006	FORMAT(1H ,8(2I4,F5.3,2X))	QUA 0750
	IZ=0	QUA 0760
23	IN=IN+1	QUA 0770
	IF(IN.GT.100)GO TO 6	QUA 0780
	I=I+1	QUA 0790
	N1(I)=NA	QUA 0800
	N2(I)=NB	QUA 0810
	A(I)=PROB	QUA 0820
	GO TO 6	QUA 0830
20	NB=N2(I)-1	QUA 0840
	IF(NB.GT.MK)GO TO 60	QUA 0850
	DO 21 N=1,I	QUA 0860
	IF(MMM(NB).NE.1)GO TO 92	QUA 0870
	IF(N1(N).EQ.0)GO TO 92	QUA 0880
C	OUTPUT EEE-TRIPLES.....	QUA 0890
	WRITE(NOTAP)NB,N1(N),N2(N),A(N)	QUA 0900
92	DO 21 K=1,I	QUA 0910
	IF(N.GE.K) GO TO 21	QUA 0920
C	CALCULATE QUADRUPLES.....	QUA 0930
	SIGN=A(N)*A(K)	QUA 0940
	ASIGN=ABS(SIGN)	QUA 0950
	IF(ASIGN.LT.AMIN)GO TO 21	QUA 0960
C	OUTPUT QUADRUPLES.....	QUA 0970
	WRITE(IOTAP)N1(N),N2(N),N1(K),N2(K),SIGN	QUA 0980
24	ND=ND+1	QUA 0990
22	FORMAT(1H ,4I5,F10.2)	QUA 1000
21	CONTINUE	QUA 1010
	IF(NA)60,5,5	QUA 1020
60	WRITE(3,999)ND	QUA 1030
999	FORMAT(1H , 'TOTAL NUMBER OF QUADS=',I9)	QUA 1040
	END	QUA 1050

APPENDIX B. A LISTING OF RELATE

```

(SUBRG,STRG):
RELATE: PROC OPTIONS(MAIN);
/* *****
RELATE: A PL-1 PROGRAM TO CALCULATE THE SIGNS OF THE E'S USING THE
QUADRUPLE PRODUCT METHOD.....L.L.MARTIN

THIS PROGRAM REQUIRES THE FOLLOWING INPUT INFORMATION:
1) ADFS-THE CUTOFF PROBABILITY-USUALLY THE SAME AS AMIN IN QUADS
2) NOES-THE LARGEST SERIAL NUMBER TO BE CONSIDERED<200
3) NTOTCY-TOTAL NO. OF CYCLES TO BE DONE
4) ITRIC-1 IF PROCEDURE CROSS IS TO BE AVOIDED-ONLY USED IN
EARLY STAGES OF A TRICLINIC SOLUTION
5) NOSI-NO. OF SIGNED E'S TO BE INPUT
THE FORMAT USED IS F(5,3),4 F(5)
THE REMAINDER OF THIS CARD AND ANY OTHER CARDS HAVE
THE SIGNED SERIAL NUMBERS OF THE INPUT E'S
WITH FORMAT N F(5)
IN ADDITION, THE TWO TAPES WRITTEN IN QUADS ARE NEEDED
***** */
DCL TITLE CHAR(80); DCL IOTAP FILE SEQUENTIAL;
DCL CARD CHAR(80);
DCL NIN(*) CTL;
DCL NOES,LA,II,JJ,NTOTCY,NIL,JA,NINA,NINB,NOSI;
DCL ARRAY(198,198) FLOAT DEC(6) EXTERNAL;
DCL AEQ,AOFS,CUM,DPROB;
DCL ABEL(7) LABEL;
DCL NCYCLES INITIAL(1);
DCL 1 QUAD,2 NA(4) FIXED BINARY(31),2 SIGN;
DCL KIND;
/* INPUT INFORMATION */
GET EDIT(TITLE)(A(80));
PUT EDIT(TITLE)(SKIP,A(80));
GET EDIT(ADFS,NOES,NTOTCY,ITRIC,NOSI)(F(5,3),4 F(5));
PUT EDIT('PROB. LIMIT=',AOFS,'NO. OF E S=',NOES,'NO. OF CYCLES=',
NTOTCY,'NO. OF INPUT SIGNS',NOSI)(SKIP,A(12),F(5,3),A(11),F(5),
A(14),F(5),A(19),F(5));
ARRAY=0.0;

```

```

RELO0010
RELO0020
RELO0030
RELO0040
RELO0050
RELO0060
RELO0070
RELO0080
RELO0090
RELO0100
RELO0110
RELO0120
RELO0130
RELO0140
RELO0150
RELO0160
RELO0170
RELO0180
RELO0190
RELO0200
RELO0210
RELO0220
RELO0230
RELO0240
RELO0250
RELO0260
RELO0270
RELO0280
RELO0290
RELO0300
RELO0310
RELO0320
RELO0330
RELO0340
RELO0350
RELO0360
RELO0370

```

```

ON ENDFILE(IOTAP) GO TO NUNEQUAL;
IF NDSI=0 THEN GO TO CYCLE;
ALLOCATE NIN(NDES);
NIN=0;
DO N=1 TO NDSI; GET EDIT(NIN(N))( F(5)); END;
CYCLE: IF NCYCLES=3 THEN GO TO CYCLE1; IF NDSI=0 THEN GO TO CYCLE1;
DO N=1 TO NDSI; DO J=N TO NDSI;
NINA=ABS(NIN(J)); NINB=ABS(NIN(N));
ARRAY(NINA,NINB)=((NIN(J)*NIN(N))/(NINA*NINB));
ARRAY(NINB,NINA)=((NIN(J)*NIN(N))/(NINA*NINB));
END;
PUT EDIT( NIN(N))(SKIP, F(5)); END;
CYCLE1: DO N=1 TO NDES; ARRAY(N,N)=1.0; END;
ST: READ FILE(IOTAP) INTO (QUAD);
/* START CALCULATION OF THE SIGNS */
DO K=1 TO 4; IF NA(K)>NDES THEN GO TO ST;
IF NA(K)=0 THEN GO TO ST; END;
DO L=1 TO 3; DO N=2 TO 4; KIND=0;
IF L>= N THEN GO TO CONT;
CALL CHECK;
IF KIND=1 THEN GO TO LABLER;
ELSE GO TO CONT;
LABLER: NIL=(L+2*N)-4;
GO TO ABEL(NIL);
ABEL(1): JA=NA(3); LA=NA(4); GO TO SIGNER;
ABEL(3): JA=NA(2); LA=NA(4); GO TO SIGNER;
ABEL(4): JA=NA(1); LA=NA(4); GO TO SIGNER;
ABEL(5): JA=NA(2); LA=NA(3); GO TO SIGNER;
ABEL(6): JA=NA(1); LA=NA(3); GO TO SIGNER;
ABEL(7): JA=NA(1); LA=NA(2); GO TO SIGNER;
ABEL(2): PUT EDIT(' ERROR IN SEARCH')(SKIP,A(16)); GO TO OUT;
SIGNER: IF ARRAY(JA,LA)=0 THEN GO TO ASSIG; BCUM=ABS(ARRAY(JA,LA));
ACUM=ABS(CUM); IF ARRAY(JA,LA)*CUM<0.0 THEN GO TO DIFFER;
DPROB=1.0-ACUM-BCUM+2.0*ACUM*BCUM;
CUM=(CUM*ACUM*BCUM)/(DPROB*ACUM);
GO TO ASSIG;
DIFFER: CUM=0;

```

```

REL00380
REL00390
REL00400
REL00410
REL00420
REL00430
REL00440
REL00450
REL00460
REL00470
REL00480
REL00490
REL00500
REL00510
REL00520
REL00530
REL00540
REL00550
REL00560
REL00570
REL00580
REL00590
REL00600
REL00610
REL00620
REL00630
REL00640
REL00650
REL00660
REL00670
REL00680
REL00690
REL00700
REL00710
REL00720
REL00730
REL00740

```

ASSIG: ARRAY(JA,LA)=CUM;	RELO0750
ARRAY(LA,JA)=CUM;	RELO0760
CONT: END; END; GO TO ST;	RELO0770
/* DETERMINATION OF SIGNIFICANCE OF E RELATIONS */	RELO0780
NUEQUAL: DO II=1 TO NOES; DO JJ=1 TO NOES;	RELO0790
IF II>=JJ THEN GO TO ELOOP;	RELO0800
AEQ=ARRAY(II,JJ); IF ABS(AEQ)>AOF5 THEN	RELO0810
/* OUTPUT OF RELATED E'S */	RELO0820
PUT EDIT(' THE SIGN OF',II,'EQUALS THE SIGN',JJ,'***',AEQ,	RELO0830
'PROBS')(SKIP, A(12),F(4),A(15),F(4),A(3),F(8,4), A(5));	RELO0840
ELSE DO; ARRAY(II,JJ)=0.0; ARRAY(JJ,II)=0.0; END;	RELO0850
ELOOP: END; END;	RELO0860
SKIP3: NCYCLES=NCYCLES+1;	RELO0870
IF ITRIC=1 & NCYCLES< NTOTCY THEN GO TO TRIC;	RELO0880
CALL PARITY;	RELO0890
IF NCYCLES>NTOTCY THEN GO TO OUT;	RELO0900
CALL CROSS;	RELO0910
TRIC: CLOSE FILE(IOTAP);	RELO0920
PUT EDIT(' END OF CYCLE',NCYCLES)(SKIP, A(14),F(5));	RELO0930
GO TO CYCLE;	RELO0940
/* CHECK: PROCEDURE FOR CALCULATING PROBABILITIES */	RELO0950
CHECK: PROC;	RELO0960
CUM=ARRAY(NA(L),NA(N));	RELO0970
CUM=CUM*SIGN;	RELO0980
IF ABS(CUM)>0.80 THEN KIND=1;	RELO0990
RETURN; END CHECK;	RELO1000
/* CROSS: PROCEDURE TO RELATE E'S EQUAL TO A COMMON	RELO1010
E BUT NOT EQUAL TO EACH OTHER */	RELO1020
CROSS: PROC;	RELO1030
DCL IA,IB,IC, ID;	RELO1040
DCL AJ,BJ,CJ,DJ,EJ,FJ,GJ;	RELO1050
DCL CRS(9); DCL NCR(9),MCR(9); DCL KKK INITIAL(0);	RELO1060
PUT EDIT('OUTPUT FROM CROSS CHECK IN CYCLE',NCYCLES)(SKIP, A(32)	RELO1070
,F(3));	RELO1080
DO IA=1 TO NOES; ID=IA+1; DO IB=ID TO NOES;	RELO1090
AJ=ARRAY(IA,IB); IF ABS(AJ)<AOF5 THEN GO TO DONE;	RELO1100
DO IC=1 TO NOES; IF IC=IA IC=IB THEN GO TO DONEA;	RELO1110

BJ=ARRAY(IB,IC); IF ABS(BJ)<AOF5 THEN GO TO DONEA;	RELO1120
CJ=ARRAY(IA,IC);	RELO1130
IF ABS(CJ)<0.01 THEN DO; CJ=0.5; GO TO BEGAN; END;	RELO1140
IF CJ*AJ*BJ <0.0 THEN DO; ARRAY(IA,IC)=0.0;	RELO1150
ARRAY(IC,IA)=0.0; ARRAY(IC,IB)=0.0; ARRAY(IC,IA)=0.0;	RELO1160
ARRAY(IB,IC)=0.0; ARRAY(IA,IC)=0.0;	RELO1170
PUT EDIT('INCONSISTENCY INCOUNTERED',IA,IB,IC)(SKIP,A(25),	RELO1180
3 F(5)); GO TO DONEA; END;	RELO1190
BEGAN:FJ=ABS(AJ*BJ); EJ=ABS(CJ); GJ=1.0-FJ-EJ+2.0*FJ*EJ;	RELO1200
IF GJ=0.0 THEN PUT EDIT(FJ,EJ,IA,IB,IC)(SKIP,2 F(5,3),3 F(5));	RELO1210
IF FJ>1.01 EJ>1.01 THEN DO; PUT EDIT(' ERROR IN CROSS ',FJ,	RELO1220
IA,IB,IC)(SKIP,A(16),2 F(6,3),3 F(5)); GO TO DONEA; END;	RELO1230
IF FJ<0.01 THEN FJ=1.0;	RELO1240
DJ=(FJ*EJ*AJ*BJ)/(GJ*FJ);	RELO1250
IF ABS(DJ)>0.98 THEN DO;	RELO1260
KKK=KKK+1;	RELO1270
ARRAY(IA,IC)=DJ;	RELO1280
ARRAY(IC,IA)=DJ;	RELO1290
IF NCYCLES>NTOTCY THEN DO;	RELO1300
NCR(KKK)=IA; MCR(KKK)=IC; CRS(KKK)=DJ;	RELO1310
IF KKK=9 THEN DO;	RELO1320
PUT EDIT((NCR(IK),'=',MCR(IK),CRS(IK),'**' DO IK=1 TO 9))	RELO1330
{SKIP,9( F(3),A(1),F(3),F(5,3),A(2))}; KKK=0; END; END; END;	RELO1340
DONEA: END; DONE: END; END; RETURN; END CROSS;	RELO1350
/* PARITY: PROCEDURE TO DETERMINE ABSOLUTE SIGNS OF EEE TYPE E'S */	RELO1360
PARITY: PROC;	RELO1370
DCL NOTAP FILE SEQUENTIAL;	RELO1380
DCL 1 EVENS,2 NNN(3) FIXED BINARY(31),2 PRD;	RELO1390
DCL JN INITIAL(0);	RELO1400
DCL INN(300,3); DCL PROD(300);	RELO1410
DCL ABCD,DET,ASUM,BOTT;	RELO1420
DCL SUM INITIAL(0.0);	RELO1430
DCL I INITIAL(1);	RELO1440
DCL CAR CHAR(1);	RELO1450
INN(1,1)=99;	RELO1460
ON ENDFILE(NOTAP) GO TO PINK;	RELO1470
RED: READ FILE(NOTAP) INTO(EVENS); IF NNN(1)>NOES NNN(1)=0 THEN	RELO1480

```

                                GO TO PINK;
IF NCYCLES=NTDTCY THEN PUT EDIT(EVENS)(SKIP,3 F(5),F(5,3));
DO K=1 TO 3; IF NNN(K)>NDES THEN GO TO RED; END; I=I+1;
INN(I,1)=NNN(1); INN(I,2)=NNN(2); INN(I,3)=NNN(3); PRD(I)=PRD;
SKIP2: IF INN(I,1)=-INN(I-1,1) THEN GO TO WORK;
BLUE: ABCD=ABS(ARRAY(INN(I,2),INN(I,3))#PRD); ASUM=ABS(SUM);
IF SUM=0.0 THEN GO TO STRIKE; IF ABCD<0.01 THEN GO TO RED;
IF SUM#ARRAY(INN(I,2),INN(I,3))#PRD>0.0 THEN
SUM=(SUM#ASUM#ABCD)/((1.0-ASUM-ABCD+2.0#ASUM#ABCD)#ASUM); ELSE
SUM=0.0; GO TO RED;
STRIKE: SUM=ARRAY(INN(I,2),INN(I,3))#PRD; GO TO RED;
WORK: IF SUM>0.0 THEN CAR='+'; ELSE CAR='-';
PUT EDIT (' THE PROBABILITY THAT', INN(I-1,1), ' IS ', CAR, ' IS',
SUM)(SKIP,A(21),F(3),A(4),A(1),A(3),F(5,3));
IF ABS(SUM)<0.99 THEN GO TO SMALL;
DO N=1 TO I-1;
DET=ARRAY(INN(N,3),INN(N,2));
IF DET=0.0 THEN DO; DET=PRD(N)#SUM; GO TO EVALU; END;
IF DET#SUM#PRD(N)<0.0 THEN DO; DET=0.0; GO TO EVALU; END;
BOT=1.0-ABS(PRD(N)#SUM)-ABS(DET)+2.0#PRD(N)#SUM#DET;
DET=(PRD(N)#DET#SUM#DET)/(BOT#ABS(DET));
EVALU: IF DET> ADFS THEN DO;
ARRAY(INN(N,3),INN(N,2))=DET;
ARRAY(INN(N,2),INN(N,3))=DET; END;
PUT EDIT(DET)(SKIP,F(6,3)); END;
SMALL: IF JN=1 THEN GO TO COMP;
INN(1,#)=INN(I,#); PRD(1)=PRD(I); I=1; SUM=0.0; GO TO BLUE;
PINK: JN=1; IF I=1 THEN I=2; GO TO WORK;
COMP: CLOSE FILE (NOTAP); RETURN; END PARITY;
OUT: END RELATE;

```

```

RELO1490
RELO1500
RELO1510
RELO1520
RELO1530
RELO1540
RELO1550
RELO1560
RELO1570
RELO1580
RELO1590
RELO1600
RELO1610
RELO1620
RELO1630
RELO1640
RELO1650
RELO1660
RELO1670
RELO1680
RELO1690
RELO1700
RELO1710
RELO1720
RELO1730
RELO1740
RELO1750
RELO1760
RELO1770
RELO1780

```

APPENDIX C. RESEARCH PROPOSALS



In this appendix are presented a few proposals of additional structure work which are of interest to the author. These are intended to be preliminary in nature and no experimental details will be given.

It would seem unlikely in solution that the bridging NTA oxygen-rare earth bonds would be formed. Instead, these coordination sites would probably be occupied by solvent molecules. The act of crystallization could well involve replacement of these solvent molecules which are then trapped in the forming lattice. It would be of interest to carry out a diffraction study of these complexes in aqueous solution to test this hypothesis. In addition, the large number of apparent hydrogen bonds would make a neutron diffraction study of interest.

Most of the rare earth compounds which have been studied by diffraction techniques have been complexes formed with highly electronegative species such as oxygen or chlorine atoms. To be better able to evaluate the role of covalent bonding, complexes formed with less electronegative ligands, such as urotropin or thiocyanate, could be studied.

Many antibiotics are of moderate molecular weight and are crystalline in nature. Therefore, they would lend well to study by diffraction techniques. In addition, many are well characterized as to their mode of inhibition of bacterial growth. Several antibiotics with similar modes

of inhibition could be selected for structural study to determine what features they have in common. Idealistically, this information could be used in the synthesis of biologically active analogs.